Measuring Light and Illumination

Interdisciplinary Summer School

Edited by Manuel Spitschan and Anna Biller

DAYLIGHT ACADEMY

15-19 August 2022, Chexbres, CH

Contents

Introduction

Contributions

Project Reports

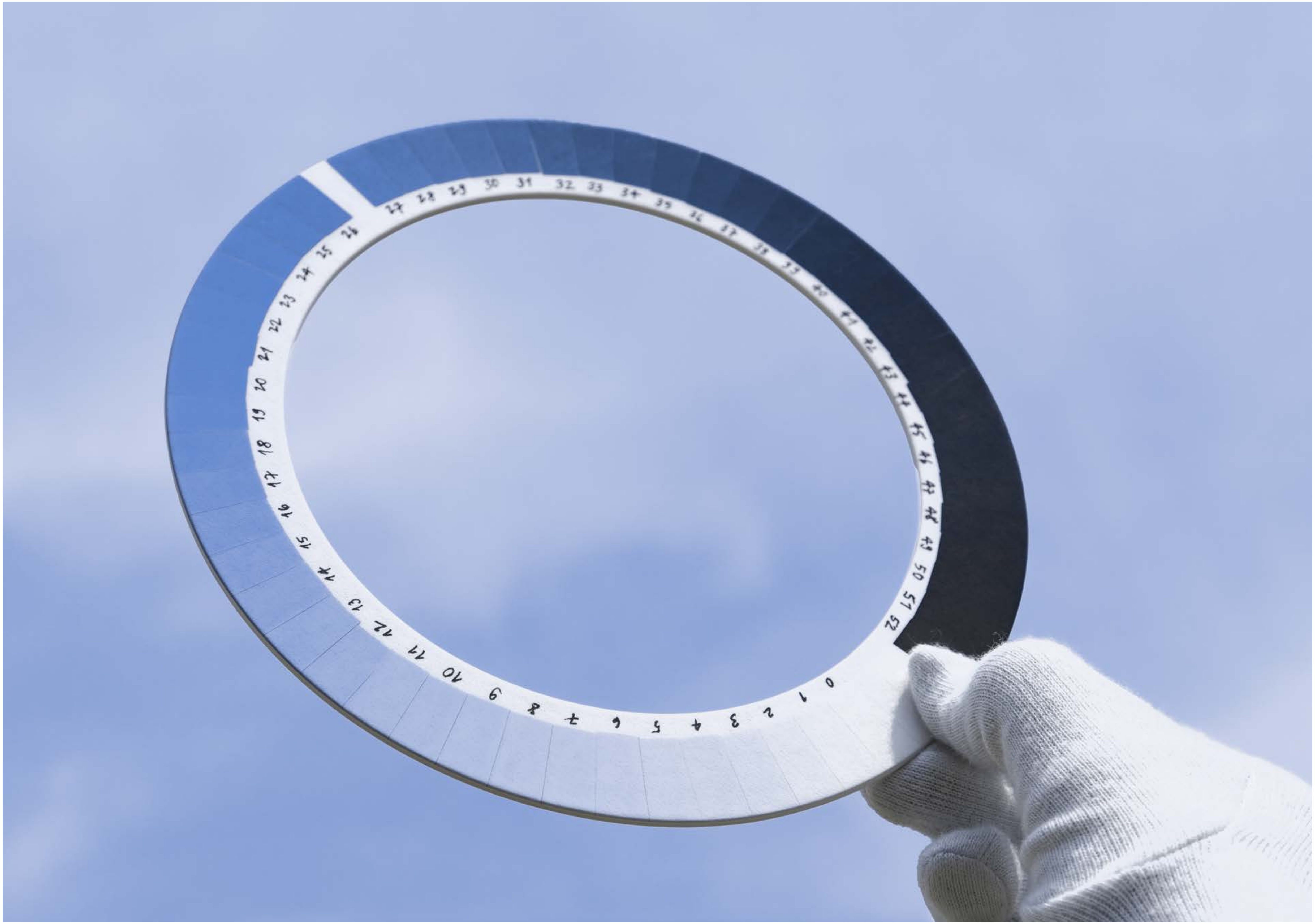

Prologue

Anna Wirz-Justice

Prologue

Anna Wirz-Justice

Let me count the ways, said the poet talking of love. Let me count the ways, says the scientist talking of light, how to measure and understand it. We see thanks to light hitting the retinal cone and rod photoreceptors. More recently, we have learned that our eyes also convey non-visual light information to the brain via specific retinal ganglion cells – to affect mood, sleep, alertness, performance, pupil size and many more physiological and biochemical phenomena. These findings have enormous consequences for understanding how the dynamics of light intensity and spectral changes across the day, as well as the timing and duration of light exposure, affect human behaviour and health. But how to measure this complexity? And who are the experts?

Because the sky is blue, it makes me cry, sang the musician. Can we update the cyanometer of Horace-Bénédict de Saussure to quantify the blueness and the blues - yet what, exactly, do we need to measure? What are the physics of blue and the emotions of blue and the aesthetics of blue? What are the differences between the dawn's early light and l'heure bleue, and are they important? An astronomer answers the child's question, why is the sky blue? as arising from the scattering, absorption, refraction of photons streaming from the sun into our atmosphere. An artist paints his beautiful arch of blue sky, an architect broadens her design palette to bring more daylight into buildings. A biomedical student worries about light sneaking into the sleeping brain: in our times, the true darkness of night has disappeared. Humans behave as though they were no longer connected to seasonal changes in night length, overridden by artificial lighting. Outdoor light pollution, indoor light pollution.

I wasn't there looking at Mont Blanc and the glistening lake of Geneva. But I can imagine the learning curve at this summer school. The mode word is interdisciplinarity, and this really was a unique cross-cultural adventure. When does one otherwise dissect a Turner painting in terms of the correlated colour temperature? Or ask, how can subjective visual perception be translated into other data sets, other scientific languages?

About the Summer School

Manuel Spitschan

About the Summer School: Teaching Light and Illumination to an Interdisciplinary Audience

Manuel Spitschan

Light and illumination influence how we live and *when we live*. Light-sensitive photoreceptors in our eyes sense light and convert it into neural impulses, allowing us to see the world, appreciate it in its colourful and moving detail, and navigate in it. These functions, which we typically summarise under "vision" or "visual perception", are mediated by the cones and rods, specialised photoreceptors to detect light at different light levels. Until the late 1990s, the cones and rods were textbook knowledge, which was challenged by the discovery of another class of photoreceptors – the so-called intrinsically photosensitive retinal ganglion cells (ipRGCs), which express the photopigment melanopsin. The ipRGCs project to the hypothalamus and mediate "non-visual" or "non-image-forming vision", including neuroendocrine and circadian responses to light.

The neurobiological discovery that light not only allows us to see but also sets our daily rhythms has significant implications for how we use light in the built environment. In practice, the imperative is to make our days brighter and our nights darker. Of course, this is not the task of neurobiologists, but of architects and lighting designers, harnessing light to yield the best effects for human physiology and behaviour. Using light optimally is therefore an *interdisciplinary* endeavour.

Between August 15th and 19th 2022, the Daylight Academy Interdisciplinary Summer School "Measuring Light and Illumination" took place in Chexbres, Switzerland, overlooking Lake Geneva. Initially, the summer school was planned for 2020 but had to be postponed due to COVID. Targeted to an interdisciplinary audience, the goal of the summer school was to truly connect the dots and provide an integrative education, solidly grounded in the technical basis of measuring light and illumination. The school brought together 17 international students, nine lecturers and three teaching assistants from various backgrounds, allowing for a space to learn about light and illumination and how to measure it. The summer school took place in the Gruppenhaus Victoria.

We found inspiration in the *cyanometer*, an 18th-century instrument developed by Horace Bénédict de Saussure (1789) to measure the colour of sky by visual inspection. Our location in Switzerland reflects where de Saussure used the instrument: On his tours onto Mont Blanc. Since 1789, our measurement of light has advanced significantly, with miniaturised spectrometers now able to capture the spectrum of light with sensors fitting on the tip of one's finger.

The result of the summer school is captured in time in this booklet. Bob **Fosbury** from the European Southern Observatory gave the keynote "How the sun paints the sky", providing a breath-taking perspective on how science and art play together and our measurement and appreciation of the colour of the sky. Christina **Hemauer** and Roman **Keller**, who ran a workshop on making cyanometers, contributed their text "Concerning the blueness of the sky". During the summer school, students worked on specific projects, and we are bringing together three contributions here.

Manuel Spitschan
Translational Sensory & Circadian Neuroscience, Max Planck Institute for Biological Cybernetics, Tübingen, Germany

TUM Department of Sport and Health Sciences (TUM SG), Technical University of Munich, Munich, Germany

TUM Institute for Advanced Study (TUM-IAS), Technical University of Munich, Garching, Germany

manuel.spitschan@tum.de

Monika **Krześniak**, Marshal **Maskarenj** and Nils **Voerste** collaborated in "Your Piece of Sky" to capture the same piece of sky using technical and artistic means, resulting in a beautiful perspective on a single "piece" of the sky. Using one of the aforementioned miniaturised spectrometers, Vaishali **Vinod** captured light exposure in time, and asked what patterns of light we are exposed to during the night, providing key pilot data for future, larger and more systematic trials. **Russo**, **Díaz-Infante**, **Liberská**, **Tabandeh**, **Loock**, **Otte**, and **Reckels** probed how light in one room – in the Gruppenhaus Victoria – varied as a function of measurement location, window opening and the use of curtains. Their report is a systematic study of how a room is not just a room – that the actual light reaching an occupant depends very much on many other parameters. Taken together, the contributions brought together in this book show the methodological breadths needed to study light and illumination.

We hope that the brochure is a testimony not only to how we can measure, understand and use light and illumination, but also to teaching it. Interdisciplinarity in practice is predicated on interdisciplinary in training and teaching. We believe that the Summer School accomplished this, and hope that it illuminates practitioners and educators alike.

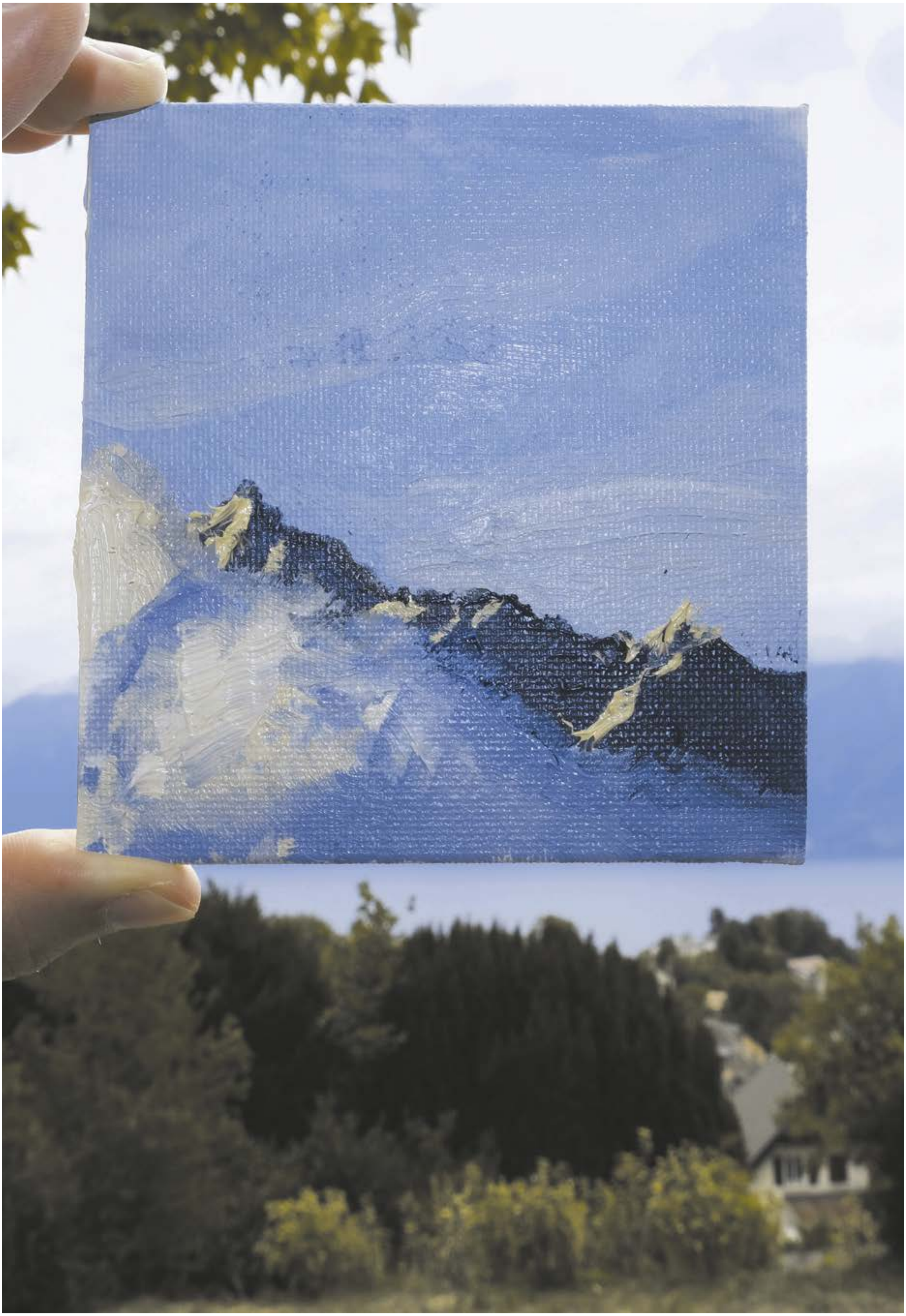

DLA Project Lead

Manuel Spitschan

Organising Committee

Anna Magdalena Biller
Christina Hemauer
Roman Keller
Lenka Maierova
Manuel Spitschan
Oliver Stefani

Faculty

Priji Balakrishnan
Peter Blattner
Christine Blume
Aicha Diakite-Kortlever
Robert Fosbury
Christina Hemauer
Roman Keller
Sabine Kling
Lenka Maierova
Björn Schrader
Manuel Spitschan

Teaching Assistant

Isabel Schöllhorn
Fatemeh Fazlali
Rafael Lazar

Participants

Alejandro Diaz Infante Rendon
Monika Krzesniak
Martina Liberská
Ann-Sophie Loock
Micaela Martinez
Marshal Maskarenj
Philip McAdams
Carla Monchen
Marzieh Nazari
Johanna Otte
Mihkel Pajuste
Samuel Ponting
Sophie Charlotte Reckels
Filomena Russo
Niloufar Tabandeh
Vaishali Vinod
Nils Voerste

Schedule

Schedule
15-19 August 2022, Chexbres, CH

Sunday 14th August

18:30			Arrival Dinner
20:00 - 21:00	*Fireside Chat*	**Introductions**	

Monday 15th August

	08:00			Breakfast
	09:00 09:30		**Welcome and Logistics**	Manuel Spitschan
Block 1: Basics and Physiology	**09:30 - 10:30**	*Lecture*	**Seeing with Cones and Rods**	Manuel Spitschan
	10:30 - 11:30	*Lecture*	**Non-Visual Effects of Light: Overview**	Oliver Stefani
	11:30 - 12:30	*Lecture*	**Effects of Light on Sleep: Why are they relevant and how can we measure them?**	Christine Blume
	12:30			Lunch
	14:00 - 15:00	*Lecture*	**Wearable Dosimetry**	Björn Schrader
	15:00 - 16:30	*Lecture*	**Measurement Overview**	
	16:30 - 18:30	*Session*	**Student Project "Bazaar"**	
	18:30			Dinner
	21:00	*Fireside Chat*	**A Lake of Illusions**	Oliver Stefani Manuel Spitschan

Tuesday 16th August

Block 2: Light in Architecture

08:00			Breakfast
09:00 - 09:30 Explanations	*Lecture*	(Il)luminance / (ir)radiance	Manuel Spitschan
09:30 - 10:30	*Lecture*	Light in Architecture	Lenka Maierova
10:30 - 11:30	*Lecture*	Variability of Daylight in Built Environments	Aicha Diakite-Kortlever
11:30 - 12:30	*Lecture*	Simulating Light and Colour in Built Environments	Priji Balakrishnan
12:30			Lunch
14:00 - 18:00	*Session*	Practical Work: Either "Bazaar" project or set project	Björn Schrader
18:30			Dinner
20:00	*Session*	Measuring the Twilight Sequence	

Wednesday 17th August

Block 3: Light in Art and Beyond

08:00			Breakfast
09:00 - 12:00	*Workshop*	Concerning the Colour of the Sky in Art	Christina Hemauer Roman Keller
12:30			Lunch
13:30 - 17:30			Free Time
18:30			Dinner
09:00 - 12:00	*Fireside Chat*	Four decades of discovery with light	Bob Fosbury

Thursday 18th August

	08:00		Breakfast
Block 4: Measurement, Metrology and Physics	09:00 - 10:00	*Lecture*	How the Sun Paints the Sky Bob Fosbury
	10:00 - 11:00	*Lecture*	Measurement of Light: Metrology and Standards Peter Blattner
	11:00 - 12:30	*Workshop*	Build your Own Spectrometer Sabine Kling
	12:30		Lunch
	14:00 - 18:00	*Session*	Practical Work: Preparation of Final Presentation
	18:30		Dinner
	20:00 - 22:00	*Session*	Presentations

Friday 19th August

	08:00		Breakfast
Block 5: Excursion to Geneva	11:00	*Transport*	Leave Viktoria to Walk to the Train Station Chexbres Village
	11:34 - 12:50	*Transport*	Train to Geneva
	13:00 - 13:50		Lunch @ Parc dela Perle du Lac
	14:00 - 15:30	*Guided Tour*	Musée d'histoire des sciences del a Ville de Genève

Contributions

Contribution 1

How the Sun Paints the Sky

Bob Fosbury

How the Sun Paints the Sky: The Generation of its Colour and Luminosity

Bob Fosbury January 2021, Abbreviated October 2022

Introduction: the 19th Century Context Science and Painting

The appearance of a brilliantly clear night sky must surely have stimulated the curiosity of our earliest ancestors and provided them with the foundation upon which their descendants built the entire edifice of science. This is a conclusion that would be dramatically affirmed if any one of us were to look upwards in clear weather from a location that is not polluted by artificial light: an increasingly rare possibility now, but one that provides a welcome regeneration of the sense of wonder.

What happened when our ancient ancestors gazed instead at the sky in daylight or twilight? It is difficult to gauge from written evidence as there was such variation in the language of description among different cultures (see "Sky in a bottle" by Peter Pesic. MIT Press, 2005. ISBN 0-262-16234-2). The blue colour of a cloudless sky was described in a remarkable variety of language, but the question of its cause most often remained in the realm of a superior being. Its nature did concern the Greek philosophers but they appeared to describe surfaces and objects in the language of texture rather than colour: they did not have a word for blue. It was only during the last millennium that thinkers really tried to get to grips with the problem, with Leonardo da Vinci, Isaac Newton and Johann Wolfgang von Goethe all applying themselves. It was not easy however, and no real progress was made until the mid-19th century when there was a focus of the greatest scientific minds of the time on the problem of both the colour and the what was then the novel property of polarisation of the light. Sir John Herschel, in 1862, remarked that these two properties were "the two great standing enigmas of meteorology". With the involvement of John Tyndall, the third Baron Rayleigh (John W Strutt), James Clerk Maxwell and subsequently Albert Einstein, he might well have used the word 'science' to replace just 'meteorology'. Herschel expressed the dilemma by pointing out that Tyndall's observations were clearly not consistent with the current theory of reflection derived by David Brewster and pointed, perceptively as it turned out, towards the need for some other explanation that would result in sunlight being reflected from air and changed in colour.

The story of cracking the problem of the blue sky is beautifully told in the book "Why is the Sky Blue" by Götz Hoeppe (English translation, Princeton University Press, 2007. ISBN2-8724-0485) who takes us up to the present day and explains how deeply entwined the story became with the concept of molecules and their sizes and numbers, reaching deep into the heart of physics and chemistry and contributing to the variety of estimates of Avogadro's number – which is related to the number and mass of atoms or molecules in a specific volume of gas.

Meanwhile, as it was gradually dawning on the scientists of the day that they might be progressing towards a major revolution in physics and chemistry and that science was not actually 'all wrapped up', the artists were getting along with painting the sky 'as it was' rather than how it was idealised.

The hugely enriched palette of colours emerging from developments in chemistry during this period enabled Turner to produce works that would shock his current audience but delight those in the future. His *Ulysses Deriding Polyphemus* (1829) was condemned as 'colouring run mad' at the time. However, both this and *The Fighting Temeraire* (1838), Fig. 1 reveal his powers of observation and perception. He could not yet rely on science for this as the latter was painted four years before the birth of Lord Rayleigh who would develop the solution to the problem raised by Tindalls' experiments and who would thus enable us to understand how the colours arise. Turner was, however, plugged into the science of the day: the Royal Academy and the Royal Society shared the same building and it seems that Turner was fascinated by science and often discussed new developments with Michael Faraday who advised him on the pigments that would survive the pollution in a smoky London.

Turner's choice of palette for the Temeraire sunset can be reproduced with a rather simple experiment using a type of glass that is easily obtained as a 'stone' cheap enough for children to buy in a gift shop. This is variously called 'opal' or 'opalescent' glass which contains tiny (really tiny) crystals of fluoride salts which have been dissolved in the glass mix and subsequently manipulated with heat treatment to result in two phases with different refractive indices (Fig. 2). The Rayleigh/Tyndall scattering of light within the glass makes an excellent analogue model of how the atmosphere produces the twilight colours in a way that will be discussed later.

Fig. 1 >

The Physical Origins of Colour in the Sky

Let us consider the origin and demise of a photon of light starting at the Sun and ending on the retina of our eye on Earth, a journey that takes only about eight minutes. If we follow as it approaches the Earth and ask what is likely to happen to it, we can begin to see what will produce the colours. The photon will not so much 'hit' the atmosphere but, in a cloudless sky, it will weave very slightly between molecules and tiny particles of liquid, dust, ice and even pollen, as it approaches the surface. These slight wiggles in path are due to the small variations in air density, and hence refractive index, that arise because of the turbulence which is the bane of astronomers' efforts to obtain sharp images from ground-based telescopes without the help of the modern adaptive-optics technology that is now becoming widely used in large telescopes.

With the Sun reasonably high in the sky and the air clear, most – but not all – of the incoming photons will reach the ground and some might even enter your eye and collaborate with a few others to trigger a photoreceptor in the retina and send a signal to the visual cortex. The colour you see after receiving a large number of photons will depend on those photons that do not make it through. Which ones are these likely to be?

The two processes that affect the photons in the atmosphere are, firstly, scattering: that is the redirection of a photon away from its original direction in space. There are several flavours of scattering, only two

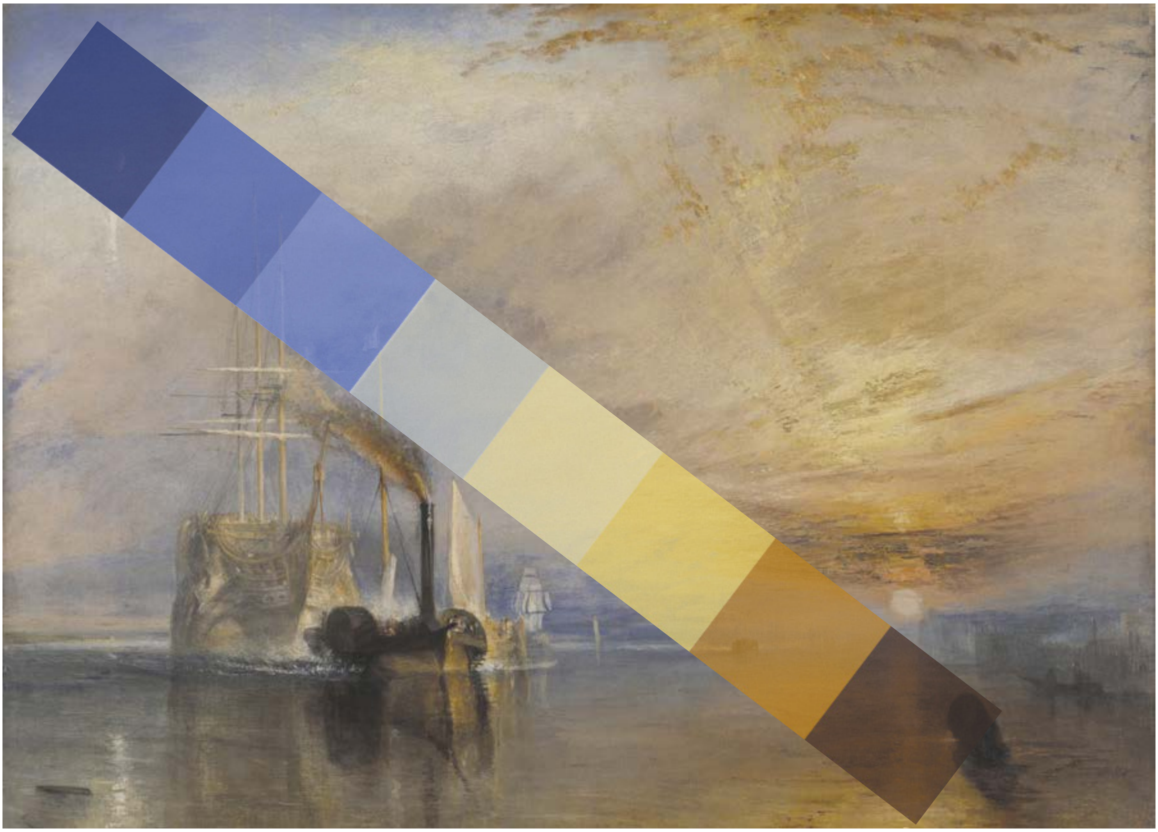

The Fighting Temeraire, tugged to her last berth to be broken up, is an oil painting by the English artist Joseph Mallord William Turner, painted in 1838 and exhibited at the Royal Academy in 1839. Turner, who was benefiting from the revolution in synthetic pigment production at the time, was interested in the science and discussed with Michael Faraday the choice of pigments that would be stable in a polluted city. The colour palette shown here was computed with an atmospheric model for twilight conditions. *Credit* Photo taken in the National Gallery with permission

of which are important for painting the sky. They are both what we call 'elastic' scattering processes which means that the redirection does not change the wavelength of the photon. Individual air molecules result in the scattering of light that Rayleigh went on to explain mathematically towards the very end of the century, and so understand the process in terms of Maxwell's theory of electromagnetism. This theory applies to scattering particles that are very much smaller than the wavelength of the light that is being scattered, in this case, molecules, mostly N2 but also O2. The characteristic of Rayleigh scattering is that it depends strongly on the wavelength of light and will scatter many more blue photons than red ones: the strength depends on the inverse fourth power of the wavelength and so blue light at 400nm will scatter 9.4 times more often than red light at 700nm. The preference for scattering blue light before red is clearly shown by Rayleigh's Fish in Fig. 3. Rayleigh's scattering theory did indeed show that Tyndall was seeing light 'reflected' from air as John Herschel had surmised!

The other scattering process is from particles that are bigger than molecules and closer to the dimension of the light wavelength. This is the case for most of the aerosols that we find in a reasonably clear atmosphere. The mathematics is more complicated than for Rayleigh and is known as Mie scattering theory after Gustav Mie who developed it early in the 20th century. For a representative mixture of aerosols found in reasonably clear air, the scattering remains stronger in the blue but the variation with wavelength is much less extreme and the blue (400nm) is stronger than the red (700nm) by just a factor of 2 with an inverse power of around 1.3 instead of the 4 for Rayleigh.

This difference between Rayleigh and aerosol (Mie) scattering allows a great richness of variation in the appearance of the sky, especially at twilight when the path length of sunlight is much longer. Differences in the density of aerosols and the natural variations in their size and shape, that cause a change in the power index away from 1.3, can vary the colour palette dramatically.

The other important difference between Rayleigh and Mie scattering is in the dependence of the scattering direction with respect to the original direction of photon travel. While the air molecules scatter approximately equally in all directions, the larger aerosols scatter most strongly in the forward direction. This is why, on a hazy day, the Sun is surrounded by a blindingly white light that can extend over an angle much larger than the solar diameter on the sky. In contrast, notice that on a very clear day, especially at high altitude, the Sun is surrounded by the only faintest of glare. Some aerosols can scatter strongly backwards as well as forwards.

What is the effect of these two types of scattering on the stream of photons arriving from the Sun? They both preferentially scatter blue light from the incoming beam of sunlight and this light is redirected to create the blue sky, but we shall return to that later. If you are on the ground bathed in sunlight, the colour will thus appear redder and somewhat fainter than it would to an astronaut on a Space Station.

The second process that lies in wait for the solar photons entering the atmosphere is called absorption. Here, the photon terminates its existence by passing its energy to an atom, molecule or particle where it is most often converted to heat. It will therefore not reach our eye but it will leave tell-tale evidence in the spectrum of skylight as what we call a *telluric* (arising from Earth) absorption line or band. There are a number of such absorption features appearing in the visible spectrum of skylight, but most of the stronger ones are near or beyond the red limit of our vision. There is one important exception however, and that results from ozone, a type of oxygen molecule that resides mostly high in the atmosphere and contains three rather than the more usual two atoms. This absorption, known as the *Chappuis* band, is very considerably weaker than the ozone absorptions that protect planetary life from damaging ultraviolet radiation, but it shows itself with increasing strength as the Sun nears the horizon and photons have to travel through a much longer atmospheric path before reaching the ground. It has a dramatic effect on the colour of the sky during twilight: it changes the daytime Rayleigh blue of a clear sky into a radically different and deeper ozone blue that is the origin of

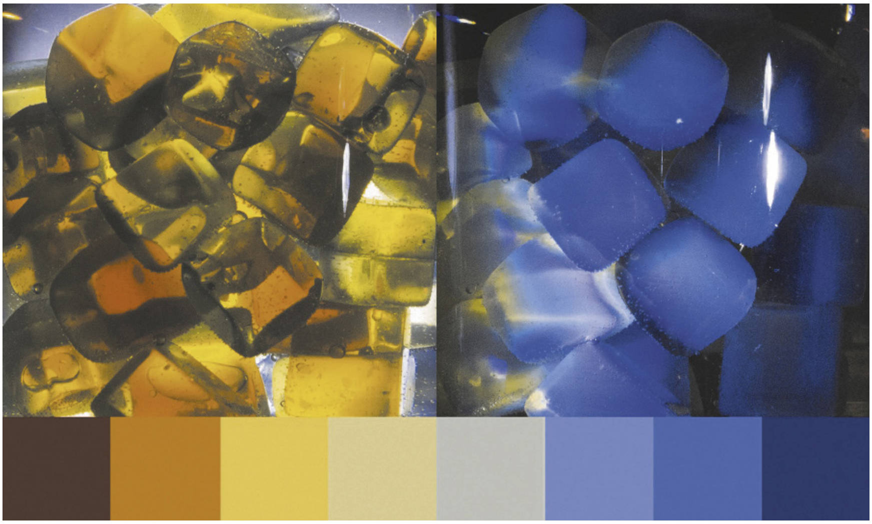

Fig. 2

Two images of a jumble of opalescent, but otherwise colourless, glass cubes in a jar containing water to reduce the refractive index difference with the surrounding medium. The image on the left is backlit with white light and that on the right is illuminated from the front right. The cubes on the left are seen mostly in transmitted light, while those on the right are scattering light towards us and seen against a dark background. The swatches along the bottom are colours computed from an atmospheric model which includes both Rayleigh and small particle (Tyndall) scattering.

Credit Fosbury/Ward/Girkin, Durham University

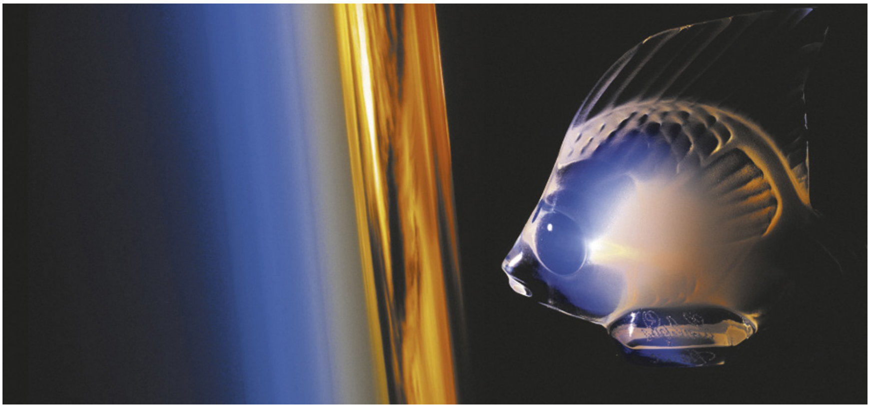

Fig. 3

Translated to a real sunset/rise seen from Earth orbit, Rayleigh's Fish (made from similar opalescent glass) gazes on our planet and considers what we now know about twilight colours. The light enters through the fish's eye and the blue light is scattered first, followed by the sequence of yellow and red.

Credit ISS photograph Credit: (NASA/ESA)

the the term *L'Heure Bleue*, The Blue Hour, used by artists to describe the special light after the Sun has set or before it rises.

The scattering blue and the ozone absorption blue act in different ways which results in the fact that the sky in daytime is only blue when it is clear. When clouds cover the sky during the day, they mix the reddened sunlight with some of the blue that has been stolen from the sunbeams and distributed over the whole sky, resulting in a grey overcast that is somewhat bluer than sunlight. At twilight however, the ozone acts like a blue filter (Fig. 4) covering the whole sky and this makes the clouds blue as well. Our eyes tend to mask this phenomenon because our visual system adapts to the changing colour, meaning that you are not as aware of this radical change to the blue light as your camera is if you switch off the 'auto white-balance'. Try it half an hour after sunset and the pictures will be so blue that you will think there must be an error!

The sum of the scattering and absorption processes acting on incoming sunlight is known as *extinction*, a term used in astronomy to represent the fraction of light from a distant object (eg. a star) reaching a telescope after traversing the atmosphere (Fig. 5). This represents the sum of the effects of scattering and absorption, both of which processes remove photons from the beam of light. The extinction of light is calculated using the Beer-Lambert-Bouger law after the three scientists who arrived at it at different times and from different applications. The mathematics is quite straightforward and easy to calculate and is based on the observation that the loss of light is proportional to the density (n) of the scatterer or absorber multiplied by the path length through the medium, the constant of proportionality being the effective cross-sectional area (σ) of the particular scatterer or absorber which will depend on wavelength. We call this product $\sigma\, n\, l$ the optical depth (τ) which is dimensionless number. Beer's law then simply states that

$$I/I_0 = e^{(-\tau)}$$

where τ represents an integral of the product along the path length, I_0 is the initial intensity and I is the incident value at the observer (Fig. 6). The complexity arises from the fact that the density of the atmosphere varies with altitude as also does the relative concentration of some of its constituents, notably water vapour and ozone. The cross-section can also vary with temperature and pressure. In practice, the equation above will contain a separate τ for every different scatterer and absorber, each with a different wavelength dependence. To see what the optical depth actually means in practice, see Fig. 7.

For our discussion of sky colours, we'll avoid doing the integrals by calling the quantity of atmosphere in a vertical column of clear air above our heads from sea level an airmass (m) of 1 which, when multiplied by the cross-section of the absorber has an optical depth of $\tau(\lambda)$ at each wavelength. The airmass can then be calculated for each solar altitude (a) from 90° at the zenith to 0° at the horizon. When the Sun is well above the horizon, the value of m can be approximated by

$$m = 1/sin(a)$$

Fig. 4 >

Closer to the horizon than about 10°, corrections need to be made because of the refraction of light in the atmosphere see: Kasten, F. and Young, A. T. (1989). "Revised optical air mass tables and approximation formula". *Applied Optics*. **28** (22): 4735–4738. The airmass to the horizon is close to 40.

The shortcoming of this simplified approach is that we assume the atmospheric gases are well mixed. While we know this not to be the case in practice we can still use the model to get quite realistic colours as

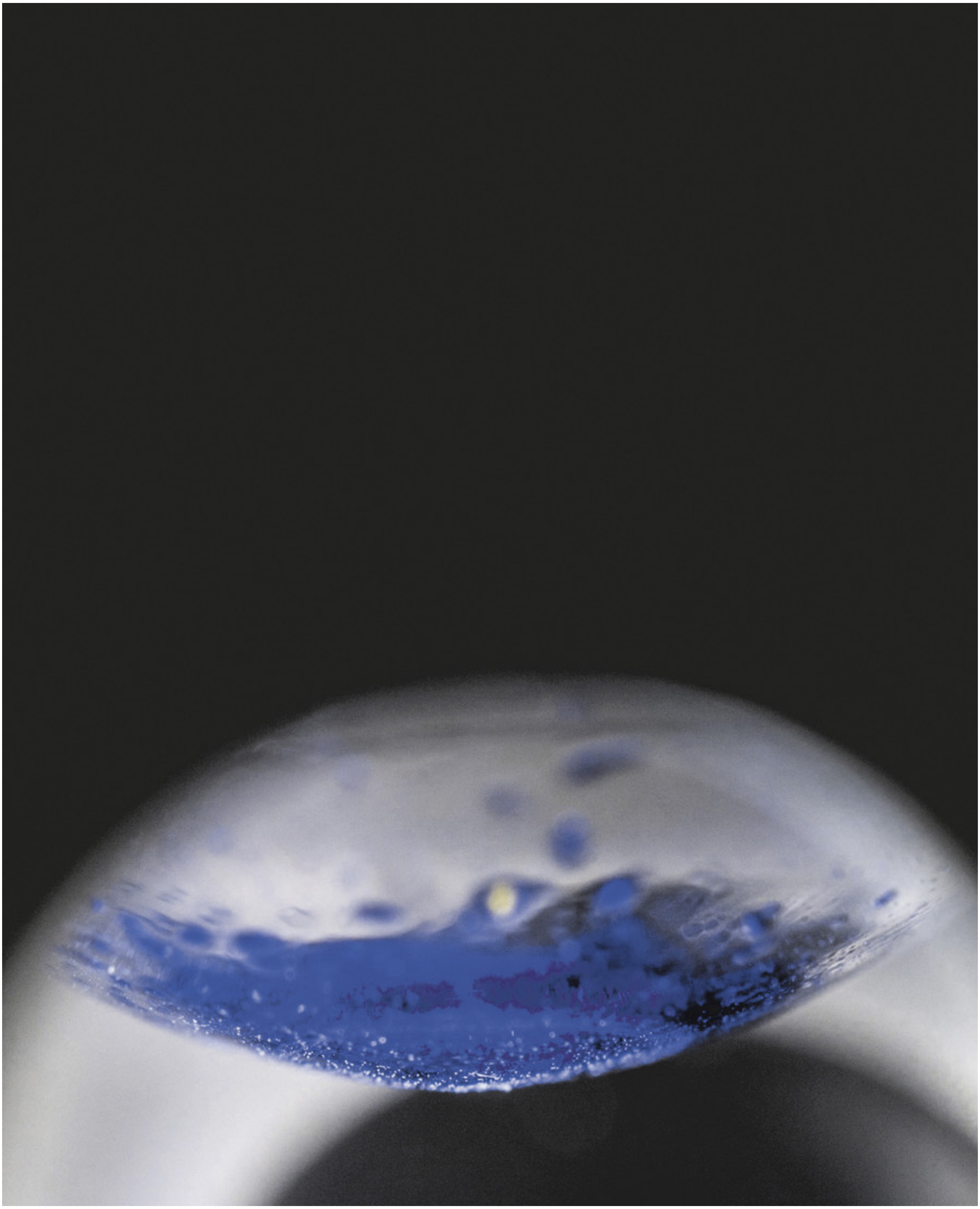

A photograph of liquid ozone showing its rich 'ultramarine' colour. This gas in the ozone layer between altitudes of about 12 and 40 km acts like a giant blue filter covering the sky at dusk and dawn. The blue colour is seen whether the sky is cloudy or not, and the physical process that causes it is entirely different from the Rayleigh scattering producing the daytime clear blue sky.

Credit Photograph courtesy of the BIPM (Bureau international des poids et mesures)

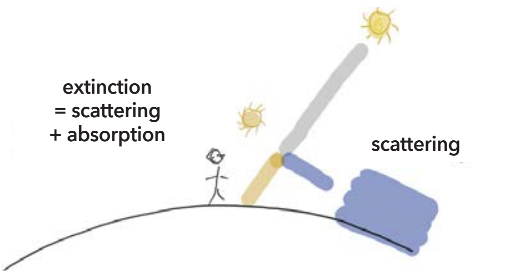

Fig. 5

The concept of extinction. As the sunlight enters the atmosphere, some of the light – predominantly blue – is scattered away from its course to form the blue sky. As the remaining light reaches ground level it appears redder to an observer there than to an astronaut seeing it from space. In addition to the scattering, some ozone absorption of orange light becomes apparent as the Sun approaches the horizon.

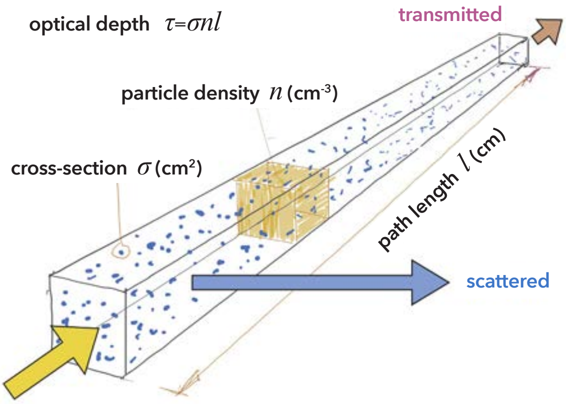

Fig. 6

Extinction and optical depth. A cartoon showing a column of air extending through the atmosphere over a path with a length l (cm). The column contains a mixture of molecules and aerosols, each with a particle density of n (cm^{-3}). The absorption or scattering cross-section (cm^2) varies with wavelength. Sunlight entering on the left (yellow arrow) will suffer extinction before leaving on the right (red arrow). Most of the extinction arises from the scattering of light away from the axis of the column (blue arrow)

Fig. 7

How does optical depth influence appearance? The left image shows a sea mist obscuring the steeply-sloping shore within a few hundred metres. Water droplets in a mist produce an extinction that it almost independent of colour and the appearance of the cliff-top around the middle of the picture represents an optical depth of about one: you can just see the cliff disappearing into the mist. In the right image, we see the setting sun through an atmosphere producing both Rayleigh and aerosol scattering. Unlike the left image where the cliff is illuminated from outside the cloud, here we see the Sun shining from way beyond the atmosphere. This means that we can still see its sharp outline through an optical depth of significantly greater than one. The atmosphere here has a high aerosol content and the optical depth ranges between a few in the red to larger than ten in the blue, making the Sun appear a deep red.

Fig. 8

What the spectrum of extinction looks like when the Sun is quite low in the sky. This plot shows as a grey line the brightness (Spectral Irradiance) of sunlight as it arrives at the top of Earth's atmosphere. The brightness is plotted on the vertical axis in units of Watts per square metre per nanometer while the wavelength, in nanometers (billionths of a metre), is plotted on the horizontal axis from the deep ultraviolet on the left to the near-infrared on the right. The red and orange lines show measurements made from close to sea level of the Sun in a clear sky. The Sun was at an altitude of 14° above the true horizon and the measurements, made with a calibrated spectro-radiometer, of the Sun alone (red line, radiance) and of the Sun and sky together (orange line, irradiance) reveal how much light has been diverted by the atmosphere. The thin blue line is the result of an extinction model using Rayleigh and aerosol scattering and ozone absorption that matches well the red line observation. In addition to the telluric absorption from ozone, marked as blue bars, the observations show the beginning of other strong telluric absorptions that extend from the deep red end of the visible spectrum through into the infrared. The three prominent bands here are due to oxygen and water molecules.

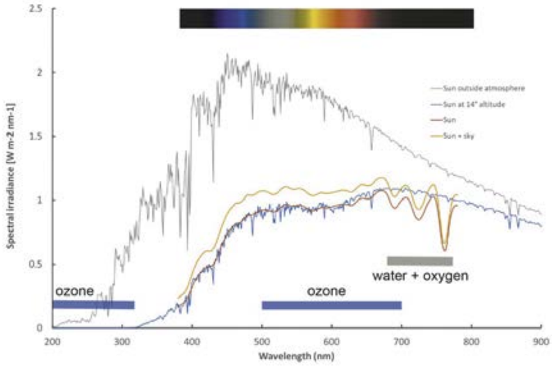

Fig. 9

Painting the bands of twilight colour. Light from the low Sun can reach us directly after suffering the extinction arising from a long, almost horizontal path through the atmosphere. It can take many alternative paths, involving a single scattering, from molecules anywhere in the atmosphere that is visible from where we are standing.

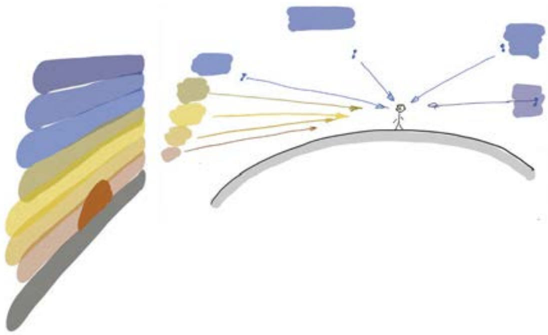

Fig. 10

In this graph, as τ increases from zero, there is a rapid rise το a maximum at τ = 1. This is followed by a slower fall as the exponential extinction begins to dominate. The effect of this behaviour is that when we look at an externally-illuminated cloud of scattering particles, most of the light reaching us from the cloud will originate in regions for which the optical depths to them from the source and from them to us has a combined value of around one. When the value of τ depends strongly on the wavelength of the light, the balance between these two opposing factors will determine which parts of the cloud (the sky) reflect (scatter) each colour we see.

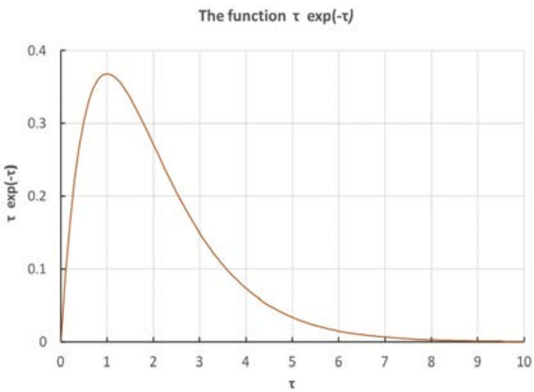

the single process of Rayleigh scattering usually dominates. To illustrate how well we can do, Fig. 8 shows the application of our extinction model (thin blue line) to an observation (red line) of the solar brightness with the Sun at an altitude of 14° above the horizon. The model only includes the two types of scattering and the ozone absorption and so does not fit the three absorption dips between about 680 and 780nm which are due to water vapour and oxygen. The radiometer used for this measurement has a low spectral resolution and does not show clearly the Fraunhofer lines in the solar spectrum.

Painting the Twilight Colours

After this discussion of the basic process of atmospheric extinction, we can move on to consider what happens to the light that has been diverted into the sky by scattering. This will allow us to see how the Sun actually does paint the beautiful bands of twilight colour (see Fig. 9).

We know how we lose sunlight by extinction. How do we calculate the light that comes to us from the sky? Imagine a beam coming from the Sun in a direction which is not directly towards us, but that will enter the atmosphere in a part of the sky that we can see from where we are. As it travels down, it will lose photons to extinction and, of those that are scattered by molecules or aerosol particles, some will come toward us, and a tiny fraction of those will enter our eye to give us an image of the sky in that direction. For each of these photons we need to know the path that it has taken during its passage through the sky. For simplicity, we will assume that it is only scattered once on its way to us. There are some regions of the sky where we need to consider multiple scatterings and that gets complicated, but the effect is small enough to ignore in this simplified discussion of colour.

That means that there are two light paths involved, one before the scattering of light coming from the Sun and one leading from the scatterer to our eye. These paths are not precisely straight. There is another effect here of some importance to astronomers. Light is bent slightly as it travels through the air towards the ground at a slant. As the density changes with altitude, the refractive effect increases, and a ray will be deflected slightly towards the region of higher density. However, the amount it bends depends on the light's wavelength and this means that the images of stars close to the horizon are stretched slightly into short spectra, with red (which bends the least) appearing to us as closer to the horizon. This shift becomes important when precise measurements of star positions are required.

The total extinction along the sequence of these two paths depends on the sum of their scattering and absorption optical depths

$$\tau_{extinction}(\lambda) = \tau_{scattering} + \tau_{absorption}$$

The second part is to determine how much light of each colour is scattered from each parcel of air along the direction to the sky where we are looking. The colour of the scattering is determined by the wavelength dependence of the scattering cross-section (bigger in the blue than in the red) which is already encoded in the optical depth

$$\tau_{scattering}(\lambda) = \tau_{Rayleigh} + \tau_{aerosol}$$

This means that the colour of light we see from any parcel of air anywhere in the sky is determined by the product of the amount of light it scatters and the total extinction. If we forget the absorption for a moment and think of a pure scattering atmosphere, this means the light we see from this piece of sky will be proportional to

$$\tau_{scattering} e^{-\tau_{scattering}}$$

We can think of these two terms as a *source* term – the brightness of light scattered from an illuminated parcel of air in the sky which **increases** with scattering strength – and a *sink* term – the light arriving after extinction which, in the negative exponential, **decreases** with scattering strength. This is the key to the beautiful bands of twilight colour! It is the balance between these two terms, one a linear increase and the other an exponential decrease, that modulates the colour over the sky. To see how this works, we just need to look at a graph of this product (Fig. 10).

If we look at a *turbid* – a scattering – medium (a glass of diluted milk, a cloud in the sky, a bank of fog, the Earth's atmosphere…) which is illuminated by an external source, the light emerging from it will come predominantly from those parts where the optical depth from the source, through the medium to our eye via a single scattering, is close to one, which is the peak of this graph.

This is illustrated in Fig. 11, which shows a sunset and a sunrise, with the Sun just below the horizon, from the Atacama desert in Chile where the sky is very often clear. If we look at the top pair of paths, we see light entering and taking an almost tangential path high through the atmosphere. If a photon scatters from a molecule high above the ground, it may scatter downwards towards our eye. Although the total length of the path taken by the photon will be long, the total amount of air – the airmass, m – will be relatively small as most of the path will be high up where the density of molecules is small (and the density of aerosols very small!). For this total path to have an optical depth of one, we have to go to a blue colour where the Rayleigh scattering is strongest. Consequently, we see the deep blue twilight sky high in the sky where the air is thinnest.

If, alternatively, we consider a beam of sunlight on a path that grazes the Earth through the dense, low atmosphere, it will travel through and scatter within a path with a much larger airmass. It will be only the orange or red photons, with their much weaker scattering, that are able to reach us from this direction: the blue light will never make it through. It is apparent that the intermediate paths between these extremes will reach this $\tau \sim 1$ balance in the sequence of subtle pastel colours between blue and red that we see in the images. The effect of absorption processes, notably ozone, is simply added to the model by adding τ_{ozone} to the optical depth term in the exponential sink term.

The presence of the ozone does have a profound effect on the colour of the twilight sky, but this happens through it acting as a filter that removes a large proportion of the orange light in a broad band that extends from the green into the red part of the spectrum. Ozone only appears as extinction (the sink) but not as a scatterer (the source). In fact, without the ozone, the deep purple-blue-grey of the twilight at the zenith above our heads would be much brighter and a pale straw-yellow/grey colour instead.

Fig. 12 shows how the colour swatches in the centre of Fig. 11 are computed by deriving RGB values for each of the computed spectra as described in the caption. The ozone extinction is included in the calculation and manifests itself as the strong broad dip centred at about 590nm.

This is, of course, a highly simplified model as the light we see is actually a combination of scatterings from parcels of air all along our line of sight. The fact that we have considered just a single parcel does not, however, make a big difference to the colours that we calculate. In reality, the colours will be mixed a little and appear slightly less saturated than in the model.

To summarise this section about the bands of colour forming in a clear sky as the Sun approaches and sinks below the horizon, let us recall that the physical processes involved are the *scattering* of light from the Sun by molecules and tiny aerosols in the atmosphere with an important contribution from *absorption* by ozone. The colour we see from a particular direction on the sky is determined by the balance between the strength of the scattering – which makes the sunlight bluer – and the extinction – which makes the light redder – including the additional effect of the absorption of orange light by ozone. This is an extraordinarily beautiful and endlessly variable phenomenon woven from just these three physical processes. To understand this in its full detail and splendour is a very complex computing problem due to the huge number of different paths the sunlight can take towards your eye from different directions and the fact that the atmosphere itself is not homogeneous but varies in temperature, density and composition with position. However, I hope that I have given you some idea about how it works to produce the colours we see.

Clouds and Shadows

A weather forecaster will usually present the prospect of clouds with a tone that suggests slight distaste and fear that their audience will greet the news with disappointment. If the resulting weather is a grey overcast, such feelings are probably quite justified. However, clouds can be spectacular (Fig. 12).

Fig. 11

A sunset and a sunrise seen from two observatories in the Chilean Atacama desert. The central column contains a set of swatches computed from a simple single-scattering atmospheric model that illustrates how the colours are formed from the passage of sunlight through different paths to an observer on the ground. The directions to the Sun in each image can be seen from the orientation of the new crescent Moon. *Credit* Y. Beletsky (LCO)/ESO

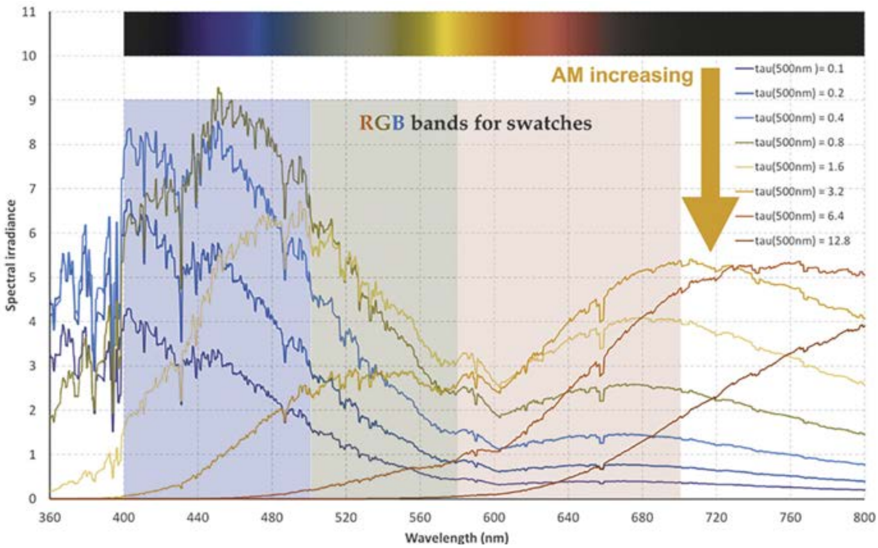

Fig. 12

A model of the sequence of twilight colours. These eight spectra were computed using the $\tau \exp(-\tau)$ formalism, with the optical depth varying from 0.1 to 12.8 at a fixed wavelength in the blue-green, to represent an increasing depth of atmosphere (airmass m) penetrated by different light paths. In these calculations, I included the effects of ozone absorption in addition to the scattering discussed in the text. The Chappuis band of ozone results in the broad spectral dip centred near 590nm. Red, Green and Blue (RGB) for each spectrum were calculated by summing the brightness within the coloured regions on the figure. These RGB values were then used to make the coloured swatches shown in Figures 1 and 11.

How are they illuminated and how do they appear with such great variety? This is not the place to write a treatise on clouds, but I will try to introduce some ideas about how they are lit and how they can influence the appearance of the sky.

What is different between clouds and clear air? Clouds contain droplets of water and/or crystals of ice in addition to gas molecules and aerosols. These droplets and crystals are generally much bigger than molecules and most aerosols, and this means that they scatter light differently.

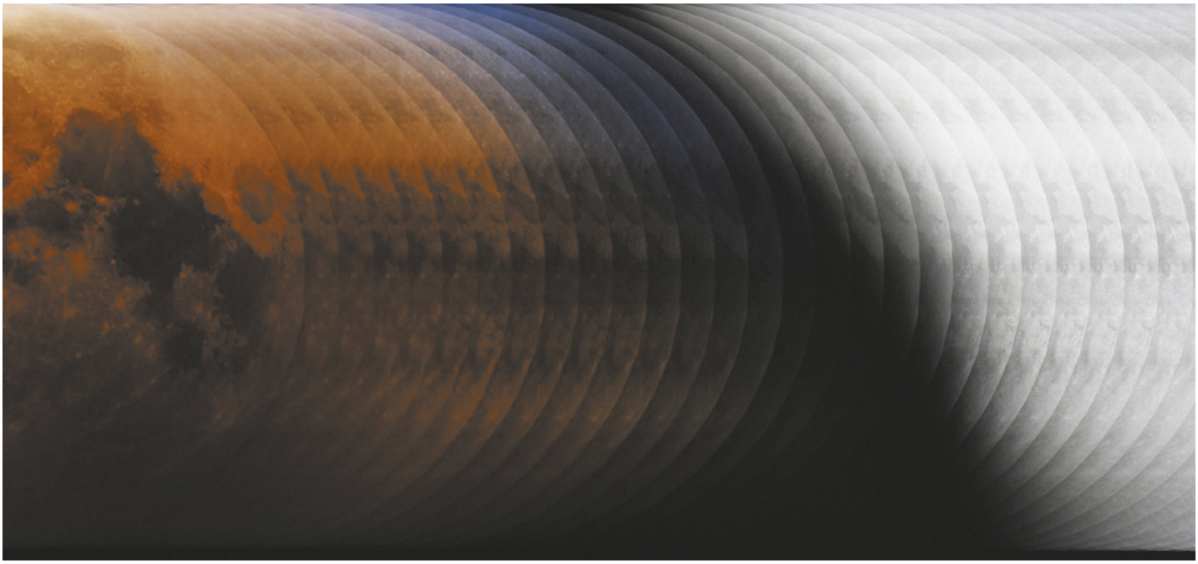

< Fig. 13

Under the shadow of a thundercloud. The distant horizon is illuminated by sunlight which reflects from the underside of the cloud. The horizontal passage of the light under the cloud is shadowed from the Sun and so does not produce the blue haze that is responsible for aerial perspective, but instead is coloured orange by the extinction. The vegetated ground will also reflect from the cloud base and acquire a green tint to our eyes – but would have a decidedly red tint if one were to use a camera sensitive to the near-infrared. Occasional lightning flashes will also be visible on the cloud (on the right of the image).

Credit Martin Kornmesser https://www.flickr.com/photos/hipydeus/50065957538/

< Fig. 14

An image of the very start of the total solar eclipse from the La Silla site of the European Southern Observatory in the Atacama Desert in Chile on 2 July 2019. The 'Diamond Ring Sun' indicates that this viewpoint is right at the edge of the shadow cast by the Moon on the Earth. On the left side we see the very distant illuminated horizon through a long shadowed path of extinction resulting in a deep orange horizon. On the extreme right however, we view a white horizon along a path which, apart from the foreground, is illuminated by sunlight which produces the additional blue haze that is responsible for the aerial perspective. Note the similarities with the thundercloud image in Figure 13.

Credit Raquel Shida, https://www.flickr.com/photos/raysinthesky/48416978517/

< Fig. 15

"Into The Shadow" by László Francsics. A stunning series of images taken during the lunar eclipse of 21 January 2019. Following the careful adjustment of the brightness by the photographer, this shows the colour produced by the extinction of a long tangential path of sunlight through Earth's atmosphere as the Moon emerges from the Earth's shadow. The path traverses successively high layers of the atmosphere until it passes through just the ozone layer and higher levels. The result is a beautiful ozone-blue. This is hard to see clearly with the eye as the blue chord of the image is much brighter than the 'blood-red' part of the Moon. *Credit* László Francsics, Astronomy Photographer of the Year 2019

As their sizes approach that of visible wavelengths, their ability to scatter strengthens and depends much less on the colour of the light so that they usually appear white or grey.

As the light enters the cloud, it scatters from droplet to droplet (or crystal). Sometimes it is absorbed and heats the cloud, but often it emerges into clear air where it escapes into space, enters another cloud or hits the ground. Consequently, not all of the light entering or emerging from a cloud comes directly from the Sun, The cloud can also 'see' the clear sky, other clouds and the ground and, under many circumstances, these sources of illumination are important: see Fig. 13 again – here the cloud sees the ground which is largely vegetated. Light from the orange sunlit horizon illuminates the lower rim of the belt of cloud around the storm. It can also be illuminated by flashes of lightning! We see all of these sources reflected from the underside of the cloud.

The other thing that a cloud does is to cast a shadow. This affects not only the ground but also the atmosphere under the cloud and has the effect of removing most of the blue haze of the aerial perspective that so influences the appearance of distant, sunlit landscapes. We see this effect under the thundercloud as the colour of the distant sunlight-illuminated horizon which appears orange because of the extinction experienced by the light from the distant sunlit clouds. Without the cloud shadow, the horizon would show a white sky and/or hazy blue mountains.

Another dramatic example of the shadow effect can be seen in the picture of the total solar eclipse shown in Fig. 14. In this case, most obvious shadow is cast not by a cloud but by the Moon onto the atmosphere during the total solar eclipse over the La Silla site of the European Southern Observatory (ESO) in the Atacama desert in Chile. The 'Diamond Ring' stage of the eclipse indicates that the picture is taken from the very edge of the Moon's shadow on the ground. The right-hand horizon appears white due to aerial perspective while the left-hand part shows a deep orange horizon without the intervening blue haze. This is a lovely illustration of the 'twilight' colours which, due to the relatively high altitude of the Sun above the horizon, are relatively free of the effects of ozone absorption.

Lunar Eclipses and Exo-Planet Transits

While a lunar eclipse in not bright enough to 'paint the sky' for us, it does paint the lunar surface in a way that echoes the mechanisms we have been discussing here. These eclipses are of special interest as the configuration of the relevant bodies in space is analogous to those during observations of the transit of an exo-planet across the face of its parent star.

Fig. 15 shows a dramatic sequence of lunar images taken during the eclipse of January 2019. The bottom left shows the deep blood-red illumination reaching the Moon from within the umbra of the Earth's shadow where the small amount of sunlight will have travelled through the lowest part of the atmosphere where it suffers an extinction which

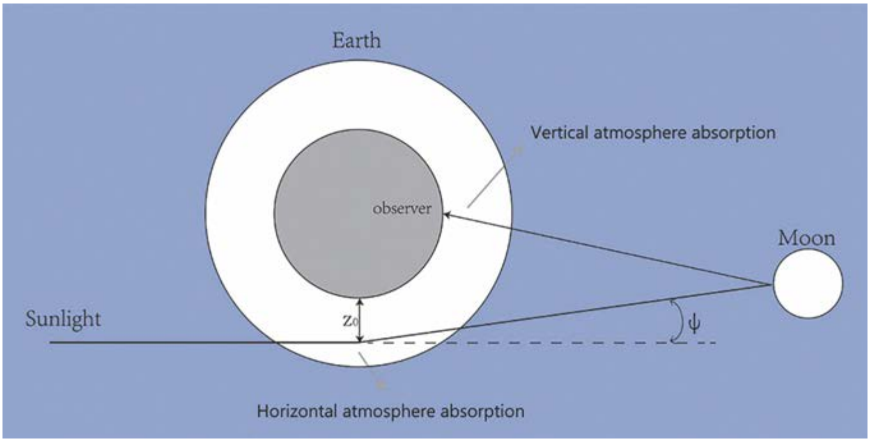

Fig. 16

Schematic of a lunar eclipse (not to scale). This shows the geometry of an eclipse where the Earth passes between the Sun and the Moon. As sunlight enters the Earth's atmosphere from the left, it gets bent slightly inwards by atmospheric refraction and then illuminates the shadowed Moon. On this long tangential path through the atmosphere, the sunlight experiences twice the amount of extinction seen at sunrise or sunset seen from the ground, and it is this reddish light that faintly illuminates the Moon. As the Moon moves out of the umbral shadow, the light path traverses successively high layers of the atmosphere until it passes through just the the ozone layer which results in the subtle and unexpected blue hues on the Moon's surface seen in Figure 15.

Credit Figure 2. from Yan et al., International Journal of Astrobiology 14 (2): 255–266 (2015)

is approximately twice that of a sunset seen from the ground. Near the top middle part of the image, the light reaching the Moon has travelled tangentially through the ozone layer which acts as a deep blue filter to produce a colour like that seen in the liquid ozone in Fig. 4. At this altitude in the atmosphere there are few aerosols and so the path is very transparent except within the orange Chappuis absorption of the ozone which results in a blue with a slight purple tint, which is the character of 'The Blue Hour' at twilight. The photographer very skilfully employed 'High Dynamic Range' (HDR) imaging techniques to capture the lovely tonal range of the phenomenon which is difficult to perceive with the naked eye due to the large differential brightness across the lunar disk.

The geometrical configuration of the three bodies involved in an eclipse is shown in Fig. 16. If we imagine the Sun being a star in another stellar system, with an exoplanet taking the place of Earth within it, and we exchange the Moon in Fig. 16 with our Earth, now a very long way away, our telescopes can observe the distant star with a tiny dot passing across its disk. The relative sizes and scales have changed but the configuration is similar. The transit will appear as a slight decrease in the star's brightness as seen by us. For an earth-like planet around a sun-like star, this change in brightness is very small, but already we can detect and measure such events with some precision. Thousands of exoplanets, most of them bigger than Earth, have been discovered in this way.

What happens to the light during such a transit? If the planet has an atmosphere, some of the light reaching us will have passed through it on the way and the light reaching our telescope will carry the imprint of the absorption spectrum of the gases within it. Can we extract the 'telluric' spectrum of the exoplanet atmosphere from this signal? The answers is yes, and it has frequently been done for planets that are significantly bigger than Earth. To do it for smaller planets will need bigger telescopes in space and on the ground and these are already being built. There are different ways of making such measurements but the way to imagine it is to look at the exaggerated thickness of the atmosphere in Fig. 16. If you were looking at this planet transiting the face of a star, the planet itself would be a black shadow and the atmosphere might be transparent for the colour of light that you were measuring. If, however, a gas in the atmosphere absorbed light at that wavelength, the atmosphere would be more opaque and the planet would appear effectively larger and obstruct more light. So all we have to do, for each wavelength in the spectrum, is to measure the amount of obstructed light and interpret that as the 'effective radius' of the planet that is causing the obstruction. How that effective radius changes with wavelength can be expressed as the absorption spectrum of the atmosphere. From that, hey presto, we identify the presence of the different gases in the atmosphere and, perhaps, ask if life has been responsible for making the mix the way it is.

It sounds quite straightforward but, as you can imagine, it is not so easy in practice. It needs very high precision measurements and very stable conditions that are extremely challenging to achieve. It has been done however, and we are getting better at it.

A way to hone the techniques is to study lunar eclipses and try to measure the constituents of the Earth's atmosphere by observing its spectrum in the faint light reflected from the surface of the Moon. There is much more light available and the Earth casts a large shadow on the Moon that we are using as part of our transit telescope. This makes it much easier to do and we learn things from this that will help to design future measurements with the new telescopes. Fig. 17 shows the result of such measurements, made during the lunar eclipse of December 2011 from near Beijing in China. For this eclipse, the grazing path of sunlight illuminating the Moon passed over the coast of Antarctica south of Australia. These observations were processed by forming the ratio of the light reflected from the Moon's surface during the eclipse to the fully illuminated Moon at the same spot on the surface after the eclipse was over. This means that the spectrum of the Sun and also the imprint of the Earth's extinction along the path from the Moon to the telescope cancel out, leaving the pure transmission spectrum resulting from the long horizontal atmospheric path over Antarctica.

This is represented by the black line spectrum at the bottom of the plot in Fig. 17. The extinction models fits for the different components of extinction appear as the coloured spectra and these include molecular (Rayleigh) and aerosol scattering and water, nitrogen dioxide and three forms of oxygen absorptions (O_2, O_3 and O_4). Note that the dominant absorber is ozone (O_3) which has a large effect on both the blue and the red colours of the eclipsed Moon: this may come as a surprise! Another surprise is the strength of the nitrogen dioxide (NO_2) absorption (the blue spectrum at the top left) which is normally considered to be a pollutant that one might not expect over the Antarctic coast. We are not sure what causes it but there are three possibilities to be considered: emissions from cruise

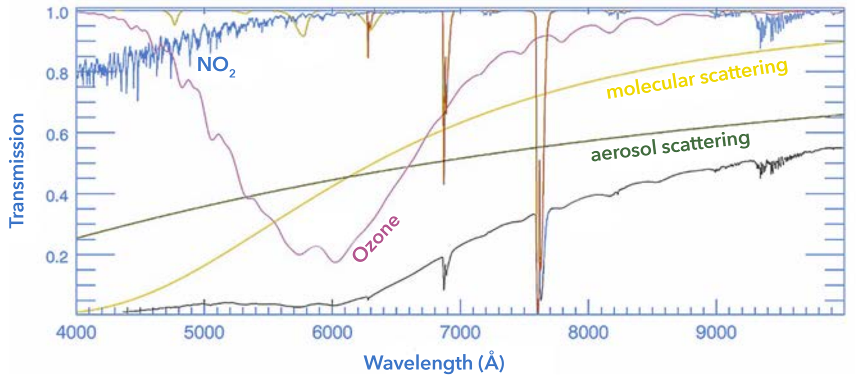

Fig. 17

Models fitted to the high resolution spectral observations made of the lunar eclipse of 10 December 2011. These show the principal scattering and absorption contributors to the extinction of sunlight reflecting from the Moon after a long passage through the Earth's atmosphere. This is analogous to the process that is used to analyse the spectroscopic observations of transiting eco-planets. The principal extinction components are aerosol and molecular scattering and water, nitrogen dioxide and three forms of oxygen absorption (O_2, O_3 and O_4). Note the very strong influence of ozone (O_3) on the colour of the eclipsed Moon.

Credit Figure 7. from "High-resolution transmission spectrum of the Earth's atmosphere-seeing Earth as an exoplanet using a lunar eclipse", F. Yan, R. A. E. Fosbury, M. G. Petr-Gotzens, G. Zhao, W. Wang, L. Wang, Y. Liu and E. Pallé. International Journal of Astrobiology 14 (2): 255–266 (2015)

ships steaming along the coast in spring, the result of nitrogen fixation over the surface of Mount Erebus which has a permanent molten lava lake at its summit and is close to the light-path or, possibly, a product resulting from the production of nitrous oxide by bacteria emerging on the Antarctic ice in spring.

Painting the Night Sky

After the twilight fades, the Sun leaves its memory in the atmosphere as the airglow mainly visible above our heads. It is difficult to see with the eye but nonetheless can be impressive and colourful in long exposure photographs. Some of the most spectacular pictures of the 'airglow' have been taken from ESO's observatories in the Atacama Desert in Chile by a band of expert 'Photo-Ambassadors' using modern digital cameras (see, eg. Link 1 https://www.eso.org/public/images/?search=Airglow). One of the images appears in Fig. 18 where the scene is some sixty million times fainter than during a clear sunny day. In conditions like this, the human eye has to rely on its rod photoreceptors which do not produce a colour signal. To see the reds and greens requires the sensitivity of the modern camera.

The airglow results from atoms and molecules that have been excited by the ultraviolet radiation from the Sun during the day but retain a reservoir of energy that can be released slowly during the following night. The phenomenon has some similarities to that of the auroræ, indeed the green and red colours come from the same pair of oxygen transitions, but the excitation and emission mechanisms differ. The glows are highly variable and make patterns that drift across the sky with the red usually being brightest shortly after sunset. There are other contributors to the airglow but they are less apparent to the eye.

Link 1 https://www.eso.org/public/images/?search=Airglow

Acknowledgement I should like to thank the organisers of these events, Manuel Spitschan and Anthony Symes, for arranging them and stimulating me to work on this topic. I am grateful to the photographers, mentioned in the credits both in this article and in the talks, who kindly allowed me to use their excellent work to illustrate this work. I especially thank David Malin who kindly made many perceptive comments which improved the clarity of the article.

^

Fig. 18

ESO's Paranal observatory in the northern Atacama Desert showing the airglow phenomenon along the horizon. Both the red and the green glow come from excited oxygen atoms slowly releasing the energy accumulated from ultraviolet sunlight during the daytime. The airglow can be seen by eye from a dark site with no Moon. However, it is too faint to trigger your cone receptors that give colour vision and you have to rely on the monochromatic rods to reveal it. Modern cameras however, are sensitive enough to reveal its full splendour.

Credit Y. Beletsky

This article was written by a scientist with a hope that it might be of some interest to artists who wish for a more physical understanding of what they see around them in the natural world. I like to think that Turner did indeed wish to understand what he was painting with such great artistic insight. Later in his century, the impressionists did get the message and started looking carefully at what was there in front of them, even learning to paint shadows as blue under the blue sky that was illuminating them! I, for one, do not think that "unweaving the rainbow" detracts from its beauty, quite the opposite!

This article is based on a talk that was given first to the Daylight Academy on 24th August 2020 (Link 2) and then to the Herschel Society on the 6th November 2020 (Link 3).

Link 2 https://www.youtube.com/watch?v=ZerHv6WY_ss&feature=youtu.be

Link 3 https://www.youtube.com/watch?v=P9v9pFluF-M&t=4329s

Contribution 2

Concerning the Blueness of the Sky

Christina Hemauer
Roman Keller

Concerning the Blueness of the Sky

Christina Hemauer; Roman Keller

Ours is an age of radical developments in humankind's relationship with – and its representations of – the natural world. Man-made climate change has come to occupy a prominent place in the perception of our existence on this planet. The following text traces the interplay between humanity and nature in and around the Alps from the beginnings of modern science and early industrialisation until now. In the interstices between the events and developments described here we encounter one area of visible change which has escaped the attention of climate science: the colour of the sky.

In the Age of Enlightenment the sky has long since stopped being a vault upon which celestial bodies are affixed. The blue colouring of the firmament remains, however, an unsolved puzzle and a popular research subject. The Genevan natural scientist Horace-Bénédict de Saussure notices that the cloudless sky grows bluer the higher one ascends. He is convinced that, "the colour of the sky can serve as a measure of the amount of opaque vapours and evaporations in the air".

Shortly before midday on the third of August 1787, Saussure and his team reach the summit of Mont Blanc [1]. The achievement is the peak of his 27-year-long involvement in expeditions. The outfit has transported an array of measuring instruments to the top of the 4,810 metre high mountain, the lightest of which is a rectangular cardboard with 16 hues. The first version of Saussure's instrument for measuring the intensity of the blueness of the sky is shown in Fig. 1.

As the son of an aristocratic family and husband to a banker's daughter, Saussure dedicates himself to a pursuit befitting his social status: science. In Geneva, devoting oneself to science is regarded as a socially respectable way of paying one's dues. In the so-called Protestant Rome, a number of natural scientists are involved in measuring the world. Accordingly, from 1768 several series of meteorological measurements

1 The first successful ascent was completed one year previously, 16 years after Saussure had offered a large reward for establishing a passable route. Jacques Balmat, who – along with Michel-Gabriel Paccard – was the first to stand on the summit in 1786, led Saussure's expedition.

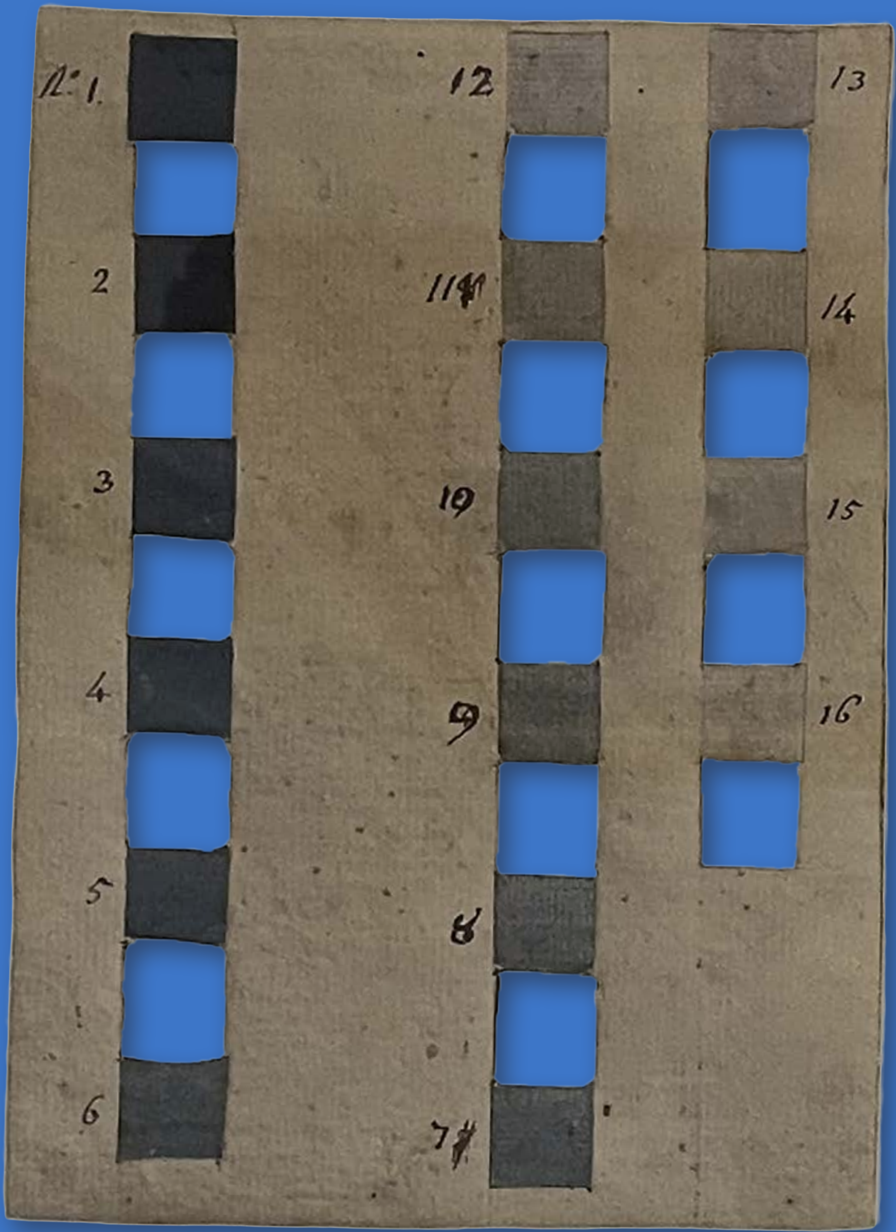

^

Fig. 1

The first cyanometer protype with 16 sections, hues ranging from dark blue to white. Musée d'histoire des sciences de la Ville de Genève.

Credit Hemauer/Keller, 2022

PREMIER MÉMOIRE

DESCRIPTION D'UN *CYANOMÈTRE* OU D'UN APPAREIL DESTINÉ A MESURER L'INTENSITÉ DE LA COULEUR BLEUE DU CIEL.

PAR M. DE SAUSSURE

Tous ceux qui ont vu d'un œil observateur les aspects dont on jouit sur les hautes montagnes, ont remarqué que le Ciel y paroît d'un bleu beaucoup plus foncé que dans la plaine. Ce phénomène m'avoit souvent frappé : lors donc que j'eus conçu l'espérance de parvenir à la cime du Mont-Blanc, je cherchai le moyen de déterminer le degré d'intensité que le Ciel me présenteroit du haut de cette cime. Je ne parvins pas alors à résoudre ce problème d'une manière générale, je me contentai donc d'emporter des papiers colorés en bleu de différentes nuances; parvenu au sommet de la montagne, je comparai ces nuances avec celle du Ciel, je mis à part la couleur qui en approchoit le plus, & cette couleur devint en quelque manière un échantillon de celle du Ciel du Mont-Blanc. Mais cela ne suffisoit pas; il falloit pouvoir rendre compte à d'autres Physiciens de l'intensité ou du vrai ton de cette couleur : il falloit même trouver une méthode générale de déterminer la nuance du Ciel dans un lieu & dans un moment quel-

Lu le 9 Mai 1790

were begun, which are still of importance for climate research today.

Following Jean-Jacques Rousseau, Saussure was a pioneer of the phenomenon Alp euphoria, which etched itself in public perceptions of nature and landscape. It did not take much longer for English painters, using Chamonix as their starting point, to discover the Alps. The representation of extreme Alpine landscapes became a discipline within European painting in its own right.

Just one year after his Mont Blanc triumph Saussure is able to quantify the correlation between the blueness of the sky and the elevation above sea level using a cyanometer he has developed. The measuring instrument is a ring-shaped cardboard disc upon which 53 strips of paper dyed in graduated shades of Prussian blue are applied [2]. On a glacier below Mont Blanc, Saussure measures the blueness of the sky at different times of day while fellow scientists simultaneously perform the same experiment in Chamonix and Geneva. At the end of his description of the experiments Saussure expresses the desire, "that the observations be replicated in different countries and climates", in order to gain insights for the field of meteorology.

Prussian blue is discovered accidentally in the early 18th century during the processing of a red dye using contaminated ingredients. Because of its brightness, non-fade and non-transparency properties, it quickly finds appeal with painters and becomes the pigment of choice in the representation of skies [3].

The cyanometer is met with keen interest by fellow researchers. Besides Johann Wolfgang von Goethe [4], Alexander von Humboldt, at the suggestion of Saussure, uses the instrument during his trip to America [5]. Humboldt's research expeditions form the basis of his five-volume magnum opus Cosmos. In this work, he attempts to provide an overview of scientific investigation concerning the natural world. He is forced to conclude, however, that the images and impressions that he experienced on his world travels elude a purely scientific description.

Man-made climate change has come to occupy a prominent place in the perception of our existence on this planet. We have unintentionally become creators of the heavens though not all to the same extent. If the measurements with Saussure's cyanometer had been conducted over a longer time frame, the change of the colour of the skies would surely have been substantiated by now. The natural scientists of the Age of the Enlightenment would have bequeathed to us an unequivocal sign that the dualism of mankind and nature has ceased to exist. Indeed, in the present day, observing the sky now involves bearing witness to the impact of human activities.

We reproduced the cyanometer 2015 as per Saussure's instructions using a series of dilutions of the colours Prussian blue and Ivory black. (Fig. 2)

2 Ivory black has been added to the darkest shades.

3 The early use of this colour is known in paintings by Antoine Watteau (1684-1721), Adrian van der Werff (1659-1722) or Canaletto (1697-1768).

4 Goethe of course extended the colour palette of the cyanometer. His colour theory, which was in his view his most important scientific contribution, turned out to be incorrect since, clinging to his ideals, he could not accept that white light consists of different colours.

5 Towards the end of his life Humboldt, in correspondence with the painter J. G. Schall, admits losing interest in the physical explanation for blueness of the sky.

For the last eight years we have been studying the colour of the sky. The aesthetic investigation went hand in hand with the question of human influence on sky colour. In cooperation with ETH climatologists, we learned that we have long since been altering the colour of the sky; that further changes are still to be determined; and that since sky colour is not considered a scientifically relevant variable, it is not observed by climate scientists.

Our research efforts range from the launch of solar balloon flights to the stratosphere in order to observe up close how colour is formed, to the construction of our own instruments for measuring sky colour, to an artistic research residency at CERN. This gave rise to numerous artworks such as Concerning the Blueness of the Sky (2015), Voyages atmosphériques (2016) or Observing Human Skies (2021), and has resulted in solo and group exhibitions in Paris, Belgrade, Mainz, Aarau and Stans as well as a growing network of collaborations with museums and institutions in Switzerland and abroad such as the Technical University of Berlin (Martine Knoop) and Munich (Manuel Spitschan).

In the workshop at the interdisciplinary summer school in Chexbres 2022, we made the offer to develop one's own cynometer. We provided the translated instructions from Saussure as well as the material we used in 2015 to reproduce the cyanometer. The task was to find a suitable dilution series for the uniform colour series. In the end, we checked the uniformity of the gradations with a commercially available spectrometer.

References

De Saussure, H. B. (1788-89). Description d'un cyanomètre ou d' un appareil destiné a mesurer l'intensité de la couleur bleue du ciel. Premier Mémoire, 409–424.

Lucius-Burckhardt-Venice-Biennale-Archive (2014).

Bartoll, J. (2008). The early use of Prussian blue in paintings. 9th International Conference on NDT of Art, Jerusalem Israel, 25–30 May. https://www.ndt.net/article/art2008/papers/029bartoll.pdf

Werner, P. (2006). Himmelsblau. Bemerkungen zum Thema „Farben" in Humboldts Alterswerk Kosmos. Entwurf einer physischen Weltbeschreibung. HiN VII, 12, 84. https://www.researchgate.net/publication/26615721_Himmelsblau_Bemerkungen_zum_Thema_Farben_in_Humboldts_Alterswerk_Kosmos_Entwurf_einer_physischen_Weltbeschreibung

Hemauer, C., & Keller, R. (2015). Communication between the climate scientist Reto Knutti and Atsumu Ohmura. https://www.hemauerkeller.land/downloads/blau/knutti-ohmura-hemkel-2015-e.pdf

Fig. 2

Concerning the human-made sky, display detail, Nidwaldner Museum.
Credit Hemauer / Keller 2022

Fig. 3

180° fisheye view on the Col du Géant (3365 m).
Credit Hemauer / Keller 2015


46
47
48
49
50
51
52
53
54
55

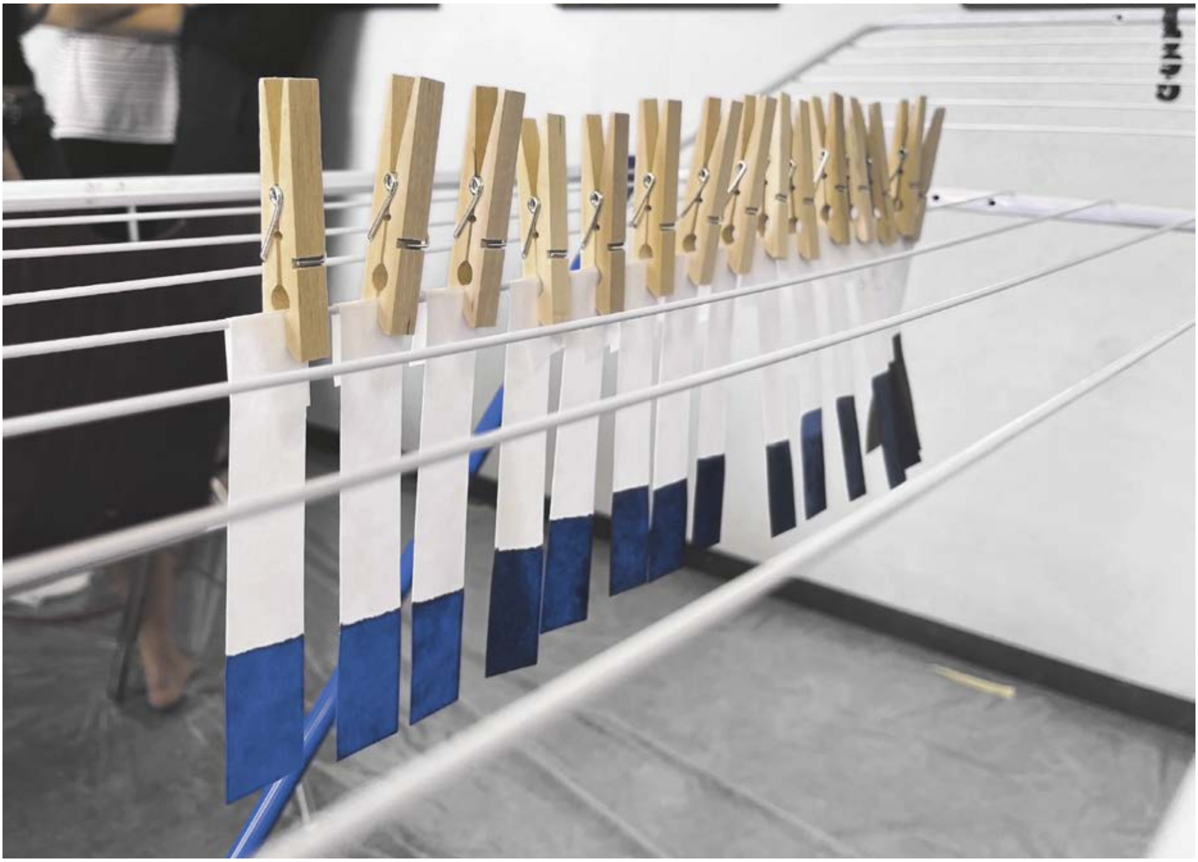



597 20.18 CET 16/8/2022 Rivaz Lake Geneva 1/100s


598 20.19 CET 16/8/2022 Rivaz Lake Geneva 1/100s


599 20.20 CET 16/8/2022 Rivaz Lake Geneva 1/100s


600 20.22 CET 16/8/2022 Rivaz Lake Geneva 1/100s


601 20.25 CET 16/8/2022 Rivaz Lake Geneva 1/60s


602 20.28 CET 16/8/2022 Rivaz Lake Geneva 1/40s


603 20.31 CET 16/8/2022 Rivaz Lake Geneva 1/25s


604 20.34 CET 16/8/2022 Rivaz Lake Geneva 1/15s


605 20.37 CET 16/8/2022 Rivaz Lake Geneva 1/13s


606 20.40 CET 16/8/2022 Rivaz Lake Geneva 1/10s


607 20.43 CET 16/8/2022 Rivaz Lake Geneva 1/8s


608 20.46 CET 16/8/2022 Rivaz Lake Geneva 1/8s


609 20.49 CET 16/8/2022 Rivaz Lake Geneva 1/5s


610 20.53 CET 16/8/2022 Rivaz Lake Geneva 1/4s


611 20.56 CET 16/8/2022 Rivaz Lake Geneva 0.4s


612 20.58 CET 16/8/2022 Rivaz Lake Geneva 0.6s

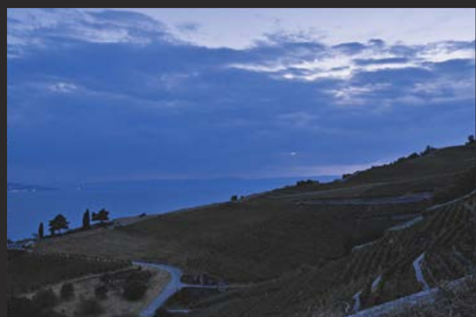
613 21.02 CET 16/8/2022 Rivaz Lake Geneva 1.3s


614 21.05 CET 16/8/2022 Rivaz Lake Geneva 2.5s


615 21.08 CET 16/8/2022 Rivaz Lake Geneva 5s

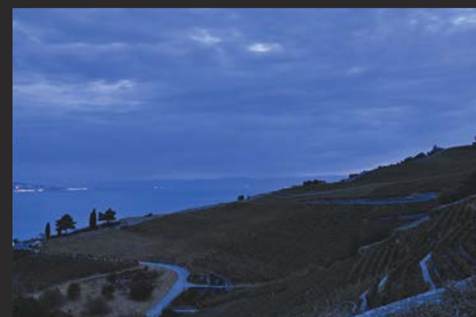
616 21.12 CET 16/8/2022 Rivaz Lake Geneva 13s

Sunset Sequence
Daylight Academy

Summer School
Chexbres

Project Reports

Project Report 1

Your Piece of Sky

Monika Krześniak
Marshal Maskarenj
Nils Voerste

Your Piece of Sky: Perception and Measurement of Daylight

Monika Krześniak; Marshal Maskarenj; Nils Voerste

Abstract

Your Piece of Sky aims to bridge the gap between subjective and objective methods of gathering data about daylight and to translate information across disciplines. The project assessed the temporal variations of daylight in colour, spectrum and intensity for a selected 'piece of sky' by comparing measurements with human perception. A piece of sky including Le Grammont and Mont-Blanc was selected during the Interdisciplinary Summer School “Measuring Light and Illumination” at Chexbres, Switzerland in August 2022. The following measurements were taken four times a day, across three consecutive days: the spot-luminance, spectral irradiance, and HDR image-based luminance maps. Through these twelve instances, the same piece of sky was painted on a 10x10cm canvas with oil paint.

A comparison based on visual appreciation between the paintings, tone-mapped HDRs, luminance maps, and representative spot colour (derived from spectral irradiance) showed similar findings between the methods. Further analysis of dominant RGB colours in the scanned paintings and the tone-mapped HDR images showed a large spread of colour coordinates on the CIE 1931 colour space. After segregation to sky and ground parts, the coordinates for the ‘sky-only’ part ranged between 5000-8000K, matching the perceived sky colour and the measurements; whereas the ‘ground-only’ parts showed greater spread in CCT. Using measured spectral irradiance data, the M/P ratio and respective CCT through the instances showed a positive correlation (R2 = 0.896), and the luminance-to-CCT relationship aligned with the research by Diakite-Knoop for the instances taken in the clear-sky conditions. A key finding was that daylight has drastic temporal variations influenced by weather and time of day, and these variations model the spatial context with different visual clarity and detail. Under photopic vision, changes in sky colours were more noticeable in paintings than in the sky’s extreme variations in luminance. This phenomenon could be explained through eye adaptation.

Introduction

Daylight, as a combination of direct sunlight and diffuse skylight, is a freely available resource contributing to occupants’ health and well-being (Wirz-Justice et al, 2021). Inspired by the names of the artworks of Olafur Eliasson with titles such as “Your light spectrum and presence” (Studio Olafur Eliasson, 2022) and by the painting series by Claude Monet “Haystacks” and “Cathedral in Rouen”, this research piece named “Your piece of sky” combined three different types of analysis of the same piece of sky. The goal of the study was to quantify the characteristics of natural light as lighting practitioners regarding ‘daylight’ (D65) as the reference for high-quality lighting (CIE, 2020). The three researchers involved in the study have different backgrounds in light and lighting; each employing a specific research method to study the same piece of sky. For an interesting collection of daylight conditions, the group studied the sky at sunrise (~07:00), solar noon (~13:30), golden hour (~20:00), and civil dusk (~21:15) times for three consecutive days.

By combining an artist's visual appreciation of daylight with measurements of luminance, colour, and spectrum, this study assessed the quality of daylit scenes through a variety of methods. The research compared measured data with a colourimetric analysis of the paintings and the tone-mapped High Dynamic Range (HDR) luminance maps, and inferences were made towards trends of correlated colour temperature (CCT) with the melanopic/photopic (M/P) ratio of different spectra and the Luminance-to-CCT correlation.

Materials and Methods

Conducted during the summer school "Measuring Light and Illumination" at Chexbres, Switzerland, this study measured luminance, spot-spectral irradiance, and high-dynamic-range (HDR) luminance map of a specific sky patch through 4 different times of day across three consecutive days (presented in Fig. 1), with a focus on the twilight periods. A patch of sky facing approximately Le Grammont and Mont Blanc was selected (demonstrated in Table. 1) with a cardboard frame.

Table. 1

Time of Day	Occasion	Day 1	Day 2	Day 3	Day 4
~ 07:00	Sunrise		✓	✓	✓
~ 13:30	Solar Noon		✓	✓	✓
~ 20:00	Golden Hour	✓	✓	✓	
~ 21:15	Civil Dusk	✓	✓	✓	

Time points through the 4 experimental days for collecting experimental data.

Through the different points in time for the experimental days, oil paintings were made on 10x10cm canvases highlighting the diurnal variation of the sky based on the artist's perception. Simultaneously, a spot luminance meter (Konica Minolta LS-150, 1° steradian) was used to measure the luminances of the sky and the ground patches, and the spectral radiance for the same position was measured using a spectrometer (GL SPECTIS 1.0 touch +FLICKER, in spectral radiance mode).

Simultaneously, the same piece of sky was photographed using a Fujifilm XT-10 CMOS camera mounted on a tripod. Standard dynamic range (SDR) images were taken at multiple exposures, always including an image captured at the correct exposure, an overexposed image and an underexposed image to later create a high dynamic range (HDR) image (Inanici, 2006). The same camera settings were used for each occasion with a set camera position, a set white balance calibrated with a grey card, a set sensitivity (iso 200), aperture (F11) and focal length (35mm).

Each set of standard dynamic range (SDR) images was compiled into an HDR image using a predefined camera response curve in Photosphere. For each HDR image, a luminance map was created based on an absolute luminance to RGB reference calibrated with the luminance spot meter (Inanici, 2006). Additionally, for each HDR image, a tonemapped SDR image was created using the Ward tone-mapping operator that is integrated into Photosphere.

Fig. 1

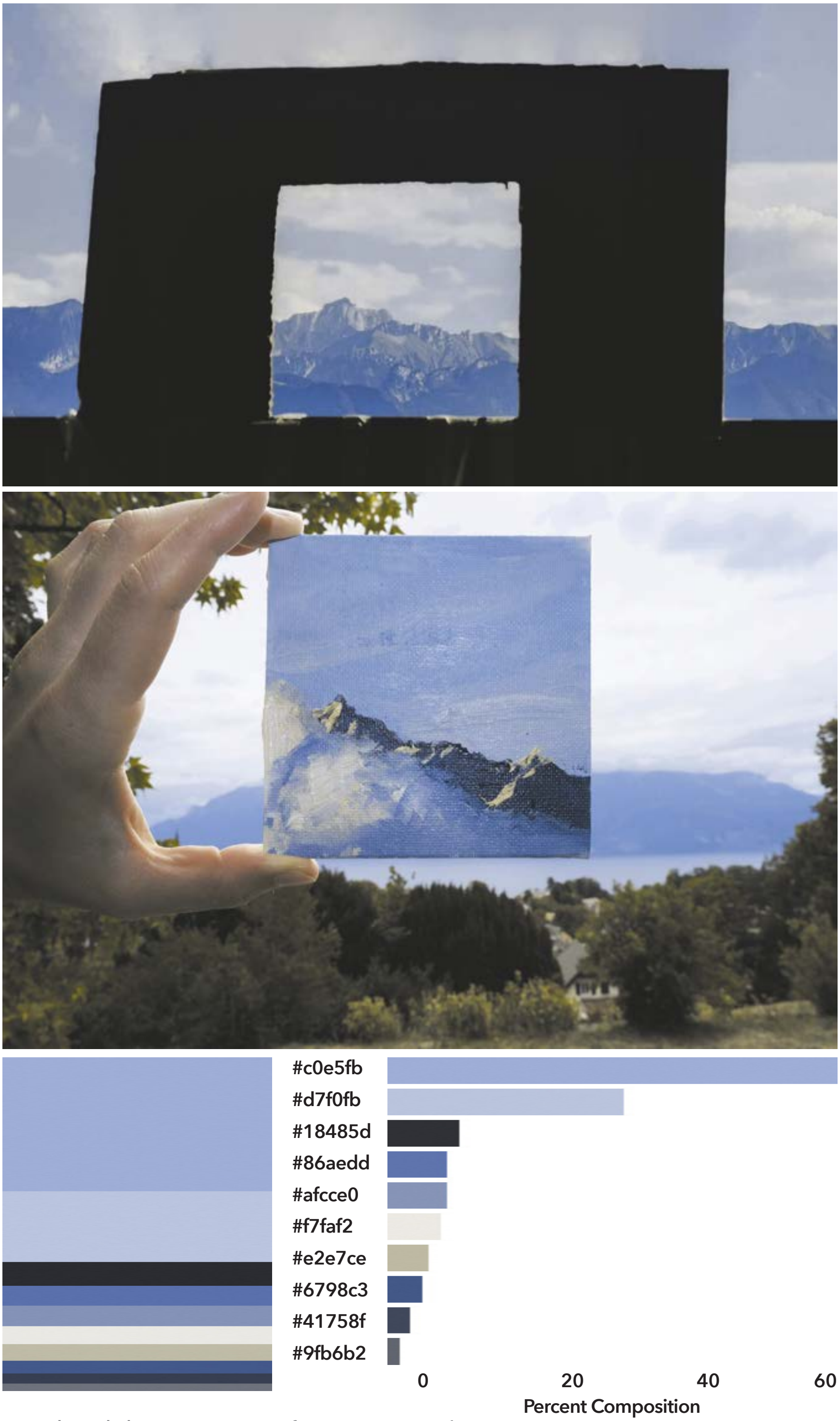

'Our piece of sky': the region of interest through these investigations, facing approximately Le Grammont and Mont Blanc, from Chexbres, Switzerland.

Credit Priji Balakrishnan

The paintings were scanned and each painting was separated into "sky-only" and "ground-only" regions using masking (Fig. 2b) – where the 'sky' regions represented pixels for the direct-sky component of perceived daylight, and the 'ground' regions represented its ground-reflected component. Using a Python SciPy script, each painting as well as its masked versions were reduced into the 10 most dominant colours (RGB) with their percentage compositions (Fig. 2c). The RGB values were then converted to CIE xyY coordinates (and CCT) using Lindbloom's CIE colour calculator (Lindbloom, 2012) (Reference White: D65, RGB model: sRGB, Adaptation: None), and these 10 most significant colours (9 in the case of the masked paintings, ignoring the most-significant mask colour) were plotted on the CIE 1931 coordinate plot; with the circle sizes corresponding to the percentage composition of the components (Fig. 2d).

Fig. 2 >

The same approach was taken for the tone-mapped HDR images, and these were compared with the coordinates plotted for the spectrometer-measured data for each time point. Through the 12 time points, boxplots were made to understand the variance in CCT for each of the six images ('entire'-painting, 'sky'-painting, 'ground'-painting, 'entire'-tone map, 'sky'-tone map, and 'ground'-tonemapped image), and to compare the data with the CCT that was measured with the spectrometer.

For the spectral data, the incident optical radiation ($W/m^2.sr.nm$) was factored with the melanopic weighting function, and its sum generated melanopic radiance ($W/m^2.sr$). Multiplying the spectrum with the photopic function (the $V(\lambda)$ curve) generated the luminance (cd/m^2). The ratio of melanopic radiance and luminance generates the melanopic over photopic (M/P) ratio: typically the M/P ratio is >1 if the incident radiation is rich in the blue part of the spectrum, and is <1 for the red-rich spectrum. For the spectral data, the CIE x,y values were derived, and CCT was further derived using McCamy's equation (McCamy, 1992). For each of the 12 instances, the CCT was plotted against the M/P ratio to evaluate their trend.

A recent work by Diakite-Knoop (Diakite-Kortlever and Knoop, 2021) was adhered to for the luminance-to-CCT correlation, and the sky-luminance to sky-CCT was converted based on luminance thresholds. For each of the measured datasets, the sky-luminance was plotted against the respective CCT values, and the point coordinates were compared with the expected trend of the luminance-to-CCT composite models.

Observations

In terms of absolute intensity, the spectral radiance for the 'typical' solar noon data was approximately 10x that of the 'typical' sunrise and golden hour through each wavelength bin (Fig. 3a), and spectral intensities for the sunrise and the golden hour data were comparable (Fig. 3b).

Normalising the spectral data by factoring the maximum value for each case generated the relative SPD, as demonstrated in Fig. 4. It can be observed that the SPDs of the sunrise and the golden hour are rich in the blue part of the spectrum (diminished data in the 550+ nm range)

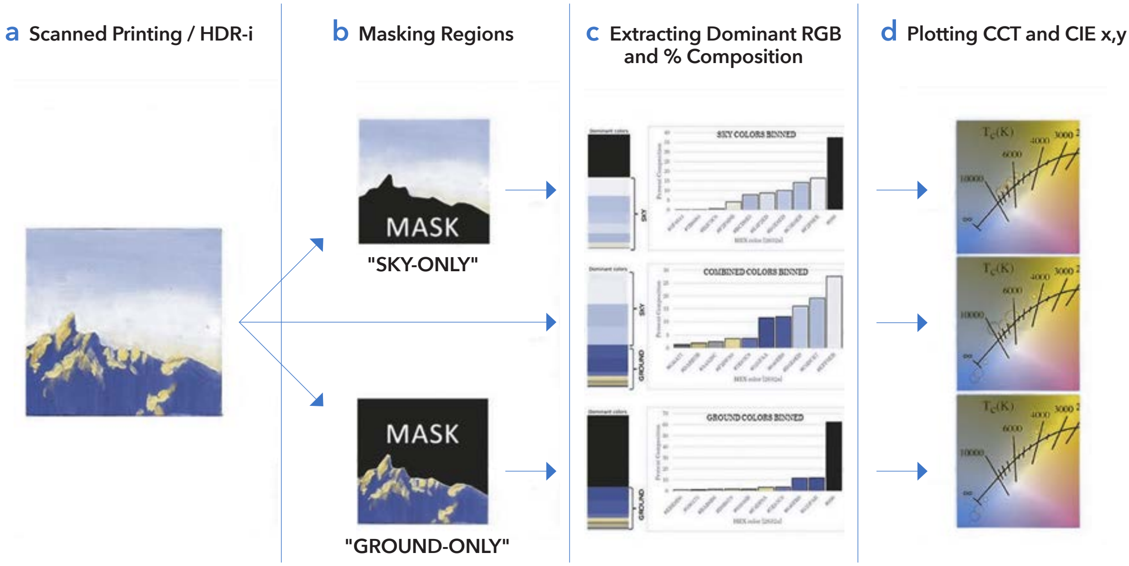

Analysis of the scanned paintings and tone-mapped HDR images: a) Original images are masked into b) 'sky-only' and 'ground-only' regions and c) dominant RGB values with per cent composition are extracted from the images and regions, and d) converted to CIE x,y and CCT and plotted on CIE 1931 coordinate plot

but the profile at solar noon shows a stronger 600-680nm range. The data shows a dip around the 590nm range for each case and reduced spectral power in the <450 and >680nm range.

Factoring the spectral data for the typical time points with the melanopic and photopic spectral sensitivity functions (Fig. 5a), it is observed that at sunrise (Fig. 5b), the melanopic peak exceeds the photopic peak, but their Areas under Curve (AUC) are approximately similar, with the melanopic daylight (D65) efficacy ratio (mDER) being 1.0179. At golden hour (Fig. 5d), the melanopic peak and AUC both exceed the photopic counterparts (mDER = 1.1313). At solar noon (Fig. 5c), the photopic peak matches the melanopic peak, but the AUC exceeds its melanopic counterpart (mDER = 0.9202). This matches the CCT captured by the spectrometer, with the sunrise being approximately the same as D65 (6412K), the spectral distribution at solar noon shifted towards red (5607K), and the spectral distribution at golden hour shifted towards blue (8062K).

The M/P ratio for the 12 instances was plotted against CCT (Fig. 6), and a positive correlation (R2 = 0.896) was achieved. By discarding an extreme data point (CCT = 19996 K, M/P = 1.49) at civil dusk, the fit was further improved (R2 = 0.9184). By plotting the CCT with luminance – both simultaneously captured by the GL Spectis spectrometer, the data were compared (Fig. 7) with the Luminance-to-CCT trend from the Berlin data (Diakite-Kortlever and Knoop, 2021), and a few points at higher luminance values taken at solar noon were observed to match the trend. However, most points did not fit the expected trend; possibly due to ground reflectance interfering with the spectral measurements.

In the post-processing of data, the scanned paintings and tone-mapped HDRs were segmented into 'sky-only' and 'ground-only' regions (Fig. 1), and their 10 most dominating RGB colours were identified (along with their percentage composition). The RGB values converted to CCT and CIE x,y were plotted on the CIE 1931 plot for each of the time points,

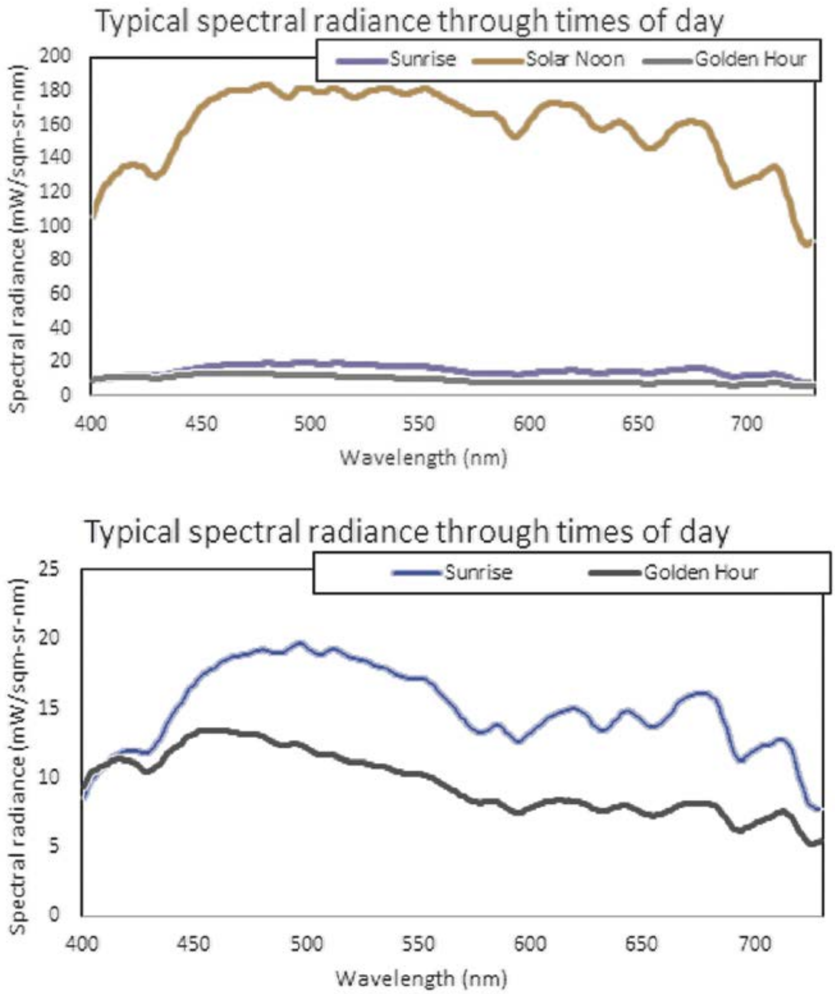

a
Sunrise
Solar noon
Golden hour

b
Sunrise
Golden hour

Fig. 3

Typical SPD through the day for (a): Sunrise, Solar Noon and Golden Hour, and (b) comparing the Sunrise with the Golden Hour

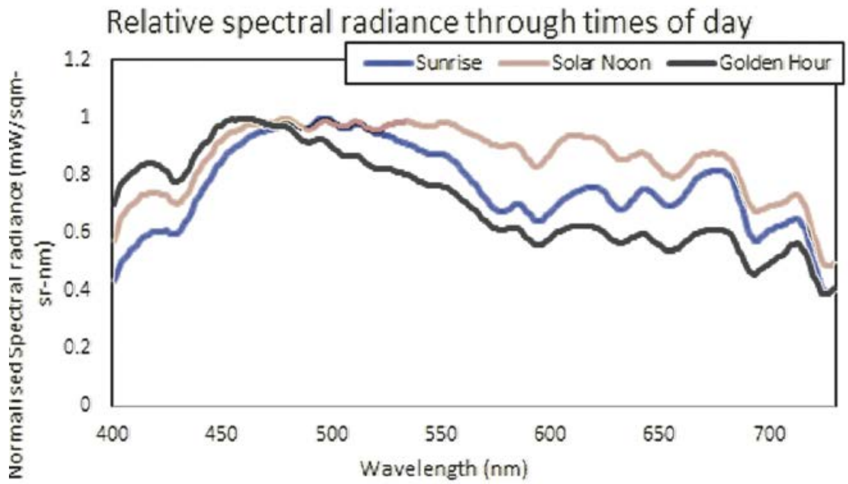

Fig. 4

Normalised relative SPD at Sunrise, Solar Noon and Golden Hour (typical data for the 3 days) a

b
mDER=1.0179, CCT= 6412K

c
mDER=0.9202, CCT=5607K

d
mDER=1.1313, CCT=8062K

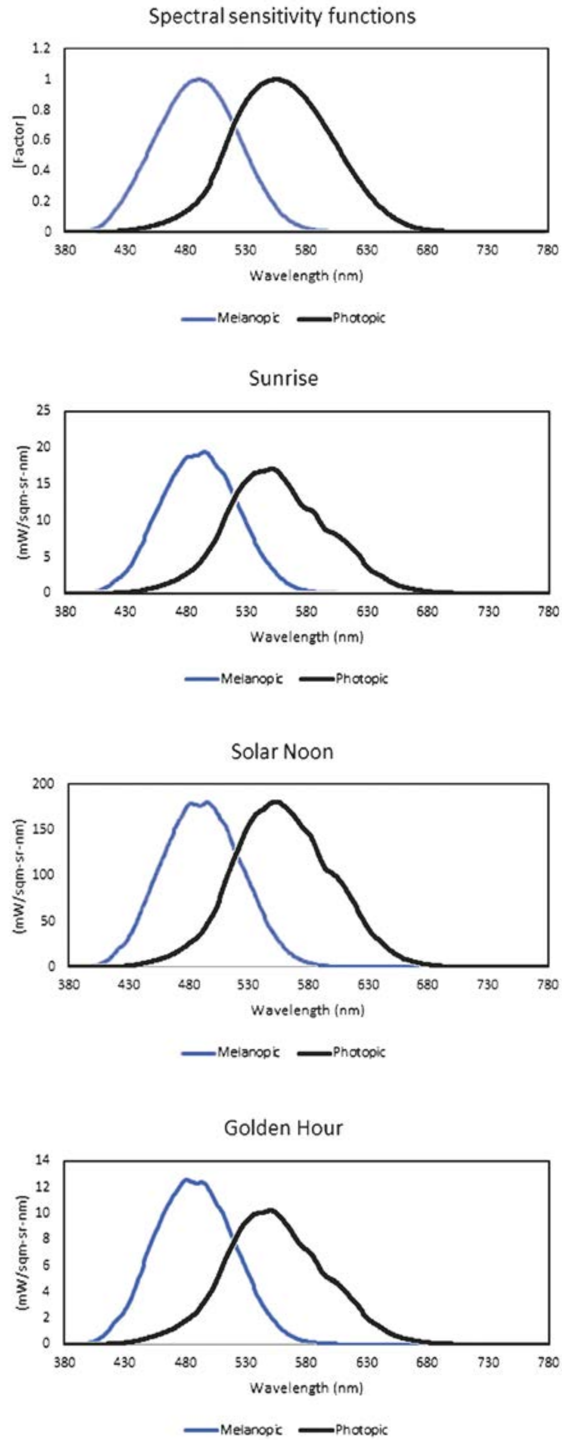

Fig. 5

Factoring the a) melanopic and photopic spectral sensitivity functions with typical SPD at(b) Sunrise, (c) Solar Noon, and (d) Golden Hour, to generate melanopic and photopic-weighted irradiances.

for masked and entire regions. For the painting of Day-2 sunrise, these plots are presented in Fig. 8.

It is observed that while the cluster for the entire painting has a large spread on the coordinate plot – with a large variance from the spectrometer-captured CCT of 6412 K, the spread reduces when the painting is analysed post-segmentation into 'sky-only' and 'ground-only' regions, with the 'sky-only' region yielding a closer fit with the spectrometer-measured CCT, and the 'ground-only' resulting in the 'too-low'/'too-high' CCT values. A similar assessment was identified in other instances as well. A boxplot of the CCT-scatter through the 6 processed images ('entire'-painting, 'sky' region of painting, 'ground' region of painting, 'entire'-tone map, 'sky' region of tone map, and 'ground' region of tone map), weighted with their percentage composition was compared with spectrometer-measured CCT and is presented in Fig. 9.

It is observed that the variance in the sky region of the tone-mapped image is minimal, followed by the variance in the sky region of the painting. There is a large variance in the ground region of the painting, also for the tone-mapped images, which contributes to the variance in the entire regions for both. In terms of mean value, the sky region of the painting has the closest mean CCT (7301 K) with the spectrometer-measured value (6412 K), and the sky region of the tone-mapped HDR image performs poorly, with a mean CCT of 4326 K. This likely occurred due to the limited colour space resulting from the fixed white balance from the first measurement set. HDR Luminance maps can be reliably used to record luminance distribution, whereas spectrometer data is more suited to record colour in a smaller sample region.

The measured spot-luminance of the sky compared with the visual appreciation of the paintings showed a great span of luminance quantities (132 cd/m2 – 13680 cd/m2) that were interpreted in the paintings as scenes of similar brightness levels (Fig. 10). This phenomenon may be explained as a result of eye adaptation (pupil dilation and constriction) to the illumination level in the environment.

On the other hand, the artist captured the slight shifts of sky colours in the paintings, which the mathematical comparison of sky colours in the painting converted to CCT with the measured CCT confirmed.

Discussion

The study has shown a correlation between the CCT values and the M/P ratio: the higher the CCT, the larger the M/P ratio. The spectral distribution curves proved to be similar at similar times of the day. At the same time, the weather conditions influenced the luminance of the natural scenes drastically and changed the luminance distribution within a matter of minutes.

The project points out the importance of eye adaptation in the visual perception of brightness. For the photopic vision, the changes in luminance in the order of 10-fold could not be seen in the record of the subjectively perceived brightness (painting). The adaptation of the eye to

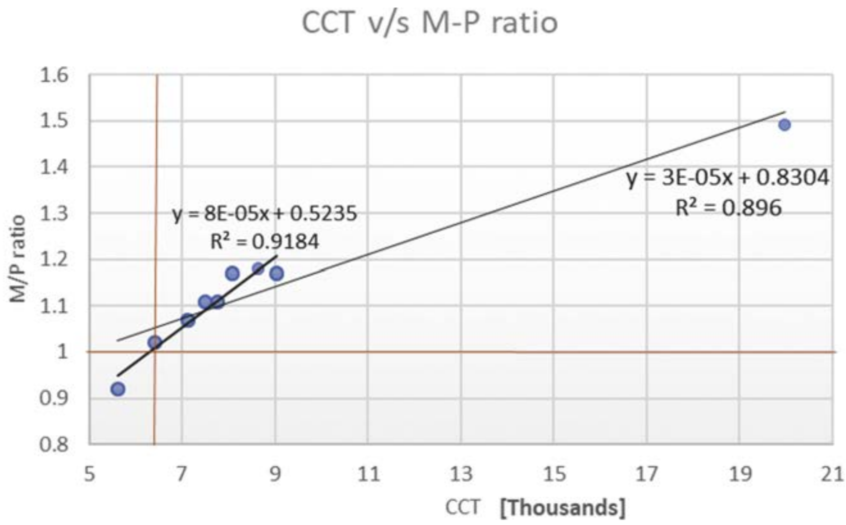

Fig. 6

Calculated melanopic over photopic ratio plotted against the CCT for the measured instances.

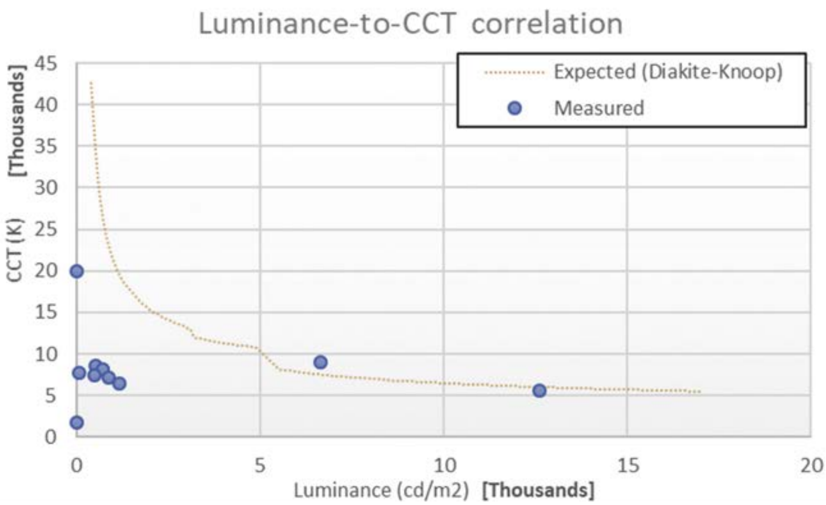

Fig. 7

Luminance to CCT correlation: comparison of simultaneously measured data with Diakite-Knoop recommendations for the luminance to CCT conversion.

different illumination of the environment should be taken into account by the designers and policymakers. By providing the right adaptation conditions, the overall light levels of the relevant environments (indoors and outdoors) could be sunk, limiting light pollution and energy consumption. Further studies are required to investigate this potential solution.

The research provokes questions of the "validity" of paintings as a source of information about human visual perception. How much of the painting was the real witness of the visual experience, and how much was changed for the aesthetical reason or due to the lack of expressive skills? The study found a good match between the "measured" and "painted" CCT values of the sky, which suggests that this method of recording visual perception is not random. Further studies might be needed to evaluate the precision of the method. An obstacle for this kind of study is the variability of painting skills amongst the population, which makes a randomised study incomparable.

As a next step, it would be interesting to record this study for

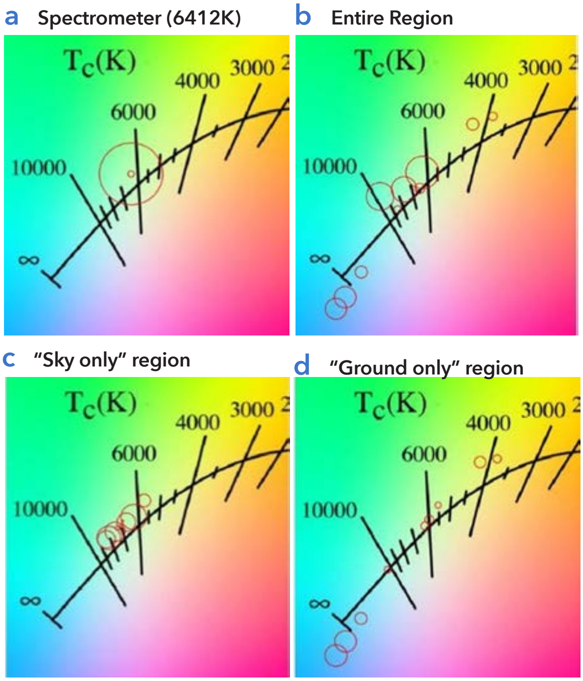

Fig. 8

Coordinate plot for (a) measured spectrum, along with the dominant RGB values-converted CIE x,y for (b) entire painting, and for the segmented (c) 'sky-only' and (d) 'ground-only' regions. Analysis presented for Day-2 sunrise painting

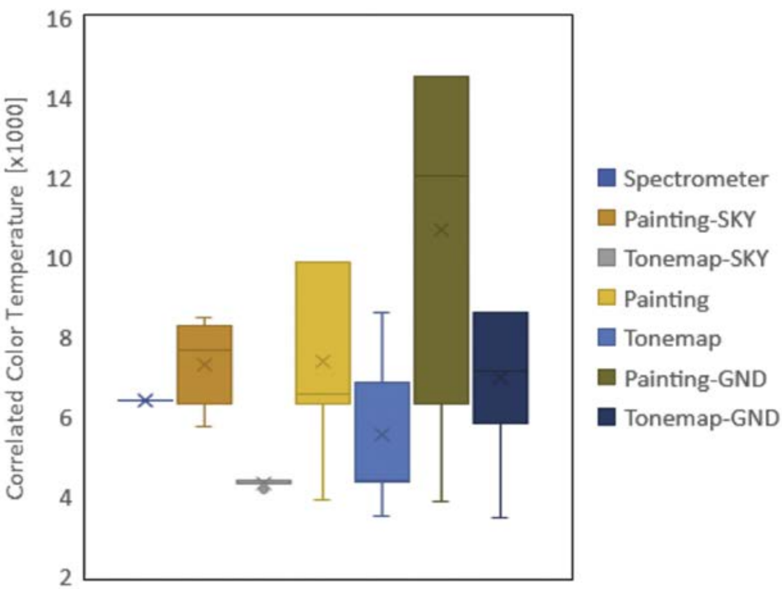

Fig. 9

CCT contributions from the three regions (entire, sky, ground) of the two image types (paintings, tone-mapped HDRs) compared with measured CCT

Fig. 10 >

Comparison between the paintings and measured spot-luminance of the reference view.

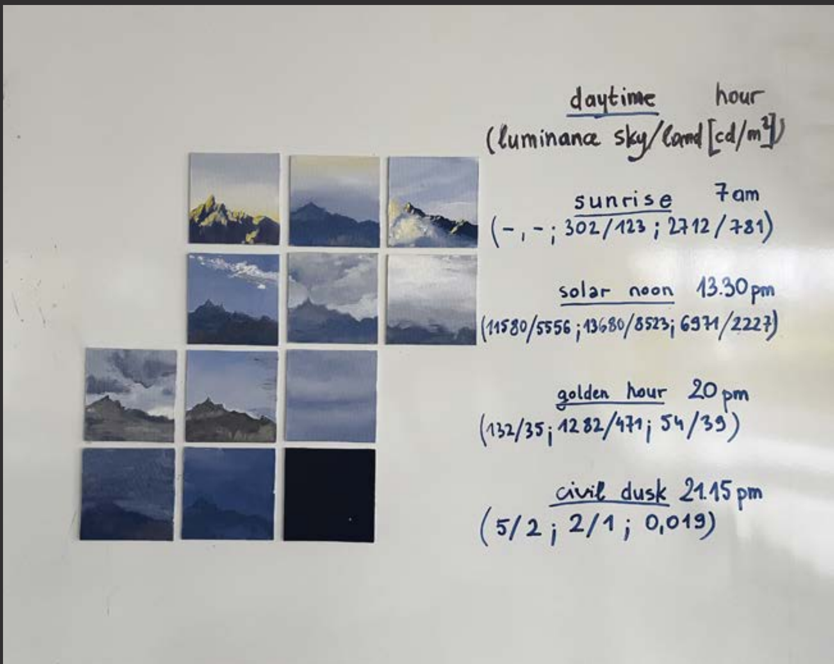
daytime hour
(luminance sky/land [cd/m²])
sunrise 7am
(–, –; 302/123; 2712/781)
solar noon 13.30pm
(11580/5556; 13680/8523; 6971/2227)
golden hour 20pm
(132/35; 1282/471; 54/39)
civil dusk 21.15pm
(5/2; 2/1; 0,019)


15. August
16. August
17. August
18. August
Sunrise (7:00h)
1026 cd/m2
482 cd/m2
302 cd/m2
123 cd/m2
2712 cd/m2
781 cd/m2
Solar Noon (13:30h)
11580 cd/m2
5556 cd/m2
13680 cd/m2
8523 cd/m2
6971 cd/m2
2227 cd/m2
Golden Hour (20:00h)
132 cd/m2
35 cd/m2
1282 cd/m2
471 cd/m2
54 cd/m2
39 cd/m2
Civil Dusk (21:15h)
5 cd/m2
2 cd/m2
2 cd/m2
1 cd/m2
0.019 cd/m2
0.019 cd/m2

longer periods (over a month or a year) and with more stable conditions (permanent set-up of painting position, camera and spectrometer). The extended study could aim at quantifying the phenomena observed in this paper.

A new set of data could include the sun angle and atmospheric conditions (aerosols and air humidity), which would help investigate the participation of the atmosphere in the colour-making process and its influence on the visibility of shapes. The broader approach would allow the researchers to trace the colour-creation process from the light source to the human eye. Such a study could contribute to the precision of the estimations of the quality of air from a painting (see Zerefos article about atmospheric effects of volcanoes depicted in paintings) (Zerefos, 2007).

Conclusion

The project Your Piece of Sky has found that research work greatly benefits from an interdisciplinary approach to the subject. By applying a mixed-method approach, the researchers tested the existing tools to translate information across disciplines (conversion of the colours in paintings and photography to CCT, luminance mapping on the photography) and included a technique to record subjective human perception of the colours and brightness in the scene (painting sketch). When the fleeting perception of the moment could be registered and compared with other data, a better understanding of the specificity of the human vision can be created.

Acknowledgement The participation of Dr Marshal Maskarenj is supported by a postdoctoral fellowship (n. 40000322) granted by the FNRS - Fonds de la Recherche Scientifique (Belgium) for the project SCALE (Shading Control Algorithms from Luminance-based Evaluations) at UCLouvain.
The authors would like to thank Prof Manuel Spitschan and the team of the summer school for guidance throughout the project and for supporting interdisciplinary research.

References

CIE. (2020). Colorimetry – part 2: CIE Standard Illuminants. CIE. https://cie.co.at/publications/colorimetry-part-2-cie-standard-illuminants

Diakite-Kortlever, A., and M. Knoop (2021), Forecast accuracy of existing luminance-related spectral sky models and their practical implications for the assessment of the non-image-forming effectiveness of daylight. Lighting Research & Technology. 2021;53(7):657-676. doi:10.1177/147715352098226

Inanici, M. (2006), Evaluation of high dynamic range photography as a luminance data acquisition system. Lighting Research & Technology, 38(2), 123–134. doi.org/10.1191/1365782806li164oa

Lindbloom, B. (2012), CIE Color Calculator. http://www.brucelindbloom.com/index.html?ColorCalculator.html

McCamy, C. (1992), Correlated color temperature as an explicit function of chromaticity coordinates. Color Research &Amp; Application, 17(2), 142-144. doi:10.1002/col.5080170211

Monet, C. Les Meules à Giverny (Haystacks series), 1888-1891 https://www.artic.edu/artists/35809/claude-monet

Monet, C. Rouen Cathedral (serie) 1892–1894 https://commons.wikimedia.org/wiki/Category:Rouen_Cathedral_by_Monet

Studio Olafur Eliasson. (2022). Artworks, Studio Olafur Eliasson. (2022). https://olafureliasson.net/archive/artwork

Weather Spark. (2022). Chexbres Climate. Weatherspark.com. Retrieved August 31, 2022, from https://weatherspark.com/y/53476/
Average-Weather-in-Chexbres-Switzerland-Year-Round

Wirz-Justice, A., D.J.Skene, and M.Münch (2021), The relevance of daylight for humans, Biochemical Pharmacology, Volume 191, 2021, 114304, ISSN 0006-2952, https://doi.org/10.1016/j.bcp.2020.114304.

Zerefos C. S., Gerogiannis V. T., Balis D., Zerefos S. C., Kazantzidis A. Atmospheric effects of volcanic eruptions as seen by famous artists and depicted in their paintings. Atmospheric Chemistry and Physics Discussions, European Geosciences Union, 2007, 7 (2), pp.5145-5172. Ffhal-00302717f. https://hal.archives-ouvertes.fr/hal-00302717/document

Project Report 2

Influence of internal shading on daylight provision, its impact on melanopic illuminance and spatial brightness perception

Russo, F
Díaz-Infante R. A
Liberská, M
Otte, J
Reckels, S.C
Tabandehsaravil, N
Loock, A-S

Influence of Internal Shading on Daylight Provision, its Impact on Melanopic Illuminance, and Spatial Brightness Perception

Russo, F.; Díaz-Infante R. A.; Liberská, M.; Tabandehsaravil, N.; Loock, A-S; Otte, J.; Reckels, S.C.

This study combines light and illumination measurements, indoors and outdoors, with emphasis on the daylight health benefits for building occupants, particularly for older age groups and those with limited access to outdoors. The study setting was a room including openable glazed windows facing south and facing west. Continuous illuminance data was recorded outdoors and indoors using data-loggers and a portable wearable device. Additional simultaneous light spectra/luminance/illuminance measurements were recorded three-times on one day, with open or closed windows and curtains.

Results highlighted the amount/quality of indoor daylight access resulting from façade orientation combined with four window and curtain configurations. Significant increased melanopic equivalent daylight illuminance (m-EDI) levels were observed with glazed windows fully open. In particular, for people limited to indoor settings, this highlights the importance of accessibility to and the adaptability of building façade components.

Key words: daylight, health, indoor m-EDI

Introduction and Background

Access to daylight has a fundamental impact on an individual's mental and physical health, in addition to aesthetic architectural design considerations. When light stimulates the human eye, it is not only converted into vision, but it also activates "non-visual" or "non-imaging" (NIF) responses. Connection between light exposure and human circadian entrainment is scientifically demonstrated; not only NIFs affect regulation of circadian rhythms, but also impact on sleep, hormones, alertness, cognitive function and mood (Cajochen, 2007; Lockley, 2010; LeGates et al, 2014; Blume et al., 2019; Vetter et al., 2022).

An estimated 55% of the world's population resides in urban areas with an expected increase to 68% by 2050 (UN, 2018). For an urban population spending 90% of their life indoors (Klepeis, 2001; WHO Europe, 2014), sufficient daylight access is a fundamental parameter for building and urban design. Lack of exposure to light during the morning can affect health and wellness (Konis, 2018). Although population ageing – a shift in a country's population distribution towards older ages (WHO, 2017) – has been observed in high income countries, WHO highlights this shift will become more dominant in low and middle-income countries by 2050. Daylight accessibility is critical to health and must be an integral part of public policies and building regulations beyond best practice guidelines present in high income countries.

The Decade of Healthy Ageing 2021-2030 (UN, 2021) encourages environments to foster conditions for current and future generations to have longer and healthier lives. If many health conditions are affected by daylight access, this is exacerbated with age: quality of life is heavily influenced by health where the aged are likely to experience several common and chronic health conditions at the same time. Sufficient levels of daylight of a certain quantity and quality must be available in spaces occupied by the elderly, mainly within their routine domestic settings where they are exposed only to a fraction of natural daylight in comparison to the outdoors; visual comfort also plays an especially significant role for the elderly. Photobiology highlights the importance of light for developing healthy environments.

Several studies have proposed different metrics to assess the effect of light on humans, of which 'melanopic equivalent daylight (D65) illuminance' (m-EDI) was adopted by the Commission Internationale de l'Éclairage (CIE) to quantify the non-visual responses to light (CIE S 026:2018). Consequently, this study sought to analyse indoor lighting variations, melanopic illuminance and wellness considering views through windows.

Objectives

The main objective of this study was to identify the difference between daylight and window-light entering the room, and to analyse the effect of indoor shading strategies with four typical domestic scenarios. The study explored how to improve visual comfort conditions indoors with the aim of finding a recommendation about available alternatives to improve visual comfort conditions in domestic settings.

Outdoors and indoors illuminances of different scenarios were compared while indoor luminance and m-EDI were characterised, with the intention of measuring how daylight access in indoor spaces is influenced by sight orientation, the adjustment of façade elements (such as windows and curtains), during different times of the day.

One of the goals was to establish a basic understanding of the extent to which positioning in the room and adjusting façade elements may modify daylight exposure indoors. The high contribution of such changes to daylight exposure could underline the importance of future interventions that target these factors aiming to improve, for example, circadian health and sleep for building occupants.

Luminance maps were used to evaluate light distribution and glare, while m-EDI informs the circadian impact of environmental illumination. Outdoor global illuminance was analysed on horizontal and vertical surfaces as a reference of daylight conditions throughout the day and performance of daylight penetration through windows.

Material and Methods

Setting

A first-floor classroom in the Gruppenhaus Victoria, in Chexbres, Switzerland [N 46.48°, E 6.77°] was selected to conduct the study. With approx. 82.8m^2 internal floor area and 2.63m floor to ceiling height, it included fourteen white tables, thirty-two chairs, and a ceiling mounted drop-down white projection screen. The room's internal finishes included: false ceiling of white modular panels with recessed light fittings, internal walls with textured off-white surface finish and medium grey vinyl smooth floor finishes. The southern and western facing façades included 1.96m high openable glazed window panels, spanning from the ceiling to windowsill level at a height of 0.67m above the finished floor level (FFL). The east facing windows were partially blocked by the projection screen and therefore were fully obscured and excluded during the indoor measurements. All windows were fitted with full height lightweight patterned curtains in white and pale earth-colours. The views towards the south overlooked Lake Geneva with mountains in the background whereas the views towards the west had trees with dense foliage some two metres away from the façade, partially blocking the west view. Fig. 1.

Scenarios and Measurements

Four different conditions were evaluated for the internal light measurements (Table. 1):

Fig. 1 >

Table. 1

Scenarios				
Condition	No.1	No.2	No.3	No.4
window glass-panels	closed	closed	closed	open
south facing curtains	open	closed	open	open
west facing curtains	open	open	closed	open

Summary of the four conditions evaluated in the room.

Metrics of visual comfort were simultaneously measured in the room (one location) and outside (three locations), to allow for comparison. Three Onset Hobo Pendant MX light data loggers (Hobo) simultaneously recorded global illuminance on horizontal and vertical surfaces outside. One 'Hobo' was positioned away from the building, in a horizontal location relatively free from obstructions. Two 'Hobos' were fixed to the building's external façade surfaces near the room's south and west facing windows. Fig. 2, Fig. 2a.

Inside the room, one 'Hobo' recorded daylight horizontal plane illuminance (on a desk surface, 0.80m above the FFL, 5m from the south wall and 2.5m from the west wall) Fig. 2, Fig. 2b. A Light-Dosimeter (LiDo) portable wearable device measured vertical illuminance facing south and melanopic equivalent daylight illuminance (m-EDI) Fig. 2, Fig. 2c. Luminance measurements inside the room at the occupant viewing point (2.5m away from the south and west building facades and at 1.2m above the FFL) were undertaken with a luminance distribution analyser Nikon D7200 CMOS 23.5 x 15.6 with fisheye lens (180° view field). Data obtained from luminance measurements were analysed in LumiDISP software via HDR pictures. Spectra data were recorded with a JETI spectraval 1501 spectroradiometer (JETI Technische Instrumente GmbH, Jena, Germany) and m-EDI was characterised through the luox tool (https://luox.app/ Spitschan et al., 2022) Fig. 2, Fig. 2d, Fig. 2e.

Results

Difference between daylight and window-light

Table. 2 compares outdoor and indoor illuminance (lux) during daytime, where the horizontal and vertical illuminance, and m-EDI are reported. Illuminance data were recorded every minute during one day, with weather conditions typically sunny and with clear sky throughout the day. The incident sunlight for interior intensity during the morning, early afternoon and early evening is reported, without the influence of

Panoramic photograph of the first-floor room

^ Fig. 2

Room layout and measuring equipment location curtains. The decrease in daylight illumination levels between indoors and outdoors is observed and was calculated to be a ratio between 1-2%.

Table. 2

	Median illuminance, lux, (range)			
	Morning 7 - 8 AM	Mid-morning 10 - 11 AM	Afternoon 2 - 3 PM	Evening 7 - 8 PM
	Median illuminance, lux, (range)			
Outdoor				
Global Illuminance (lux)	4 250	5 5111	76 226	14 126
South facade Illuminance (lux)	3 656	27 074	73 011	14 392
West facade Illuminance (lux)	1 511	3 885	19 843	3 452
Correlated Colour Temperature CCT (K)	9 574	5 442	5 531	5 269
Indoor				
Horizontal Illuminance (lux)	n.d.	555	1 076	293
Vertical Illuminance (lux), facing south	n.d.	976	1 190	243
Melanopic-EDI	n.d.	1 099	1 097	224
CCT (K)	n.d.	7 730	5 920	5 530

Outdoor and Indoor Illuminance (lux)

Vertical daylight illuminance at eye level (976 lux in mid-morning and 1190 lux in the afternoon) was higher than on the horizontal working plane (555 lux in mid-morning and 1076 lux in the afternoon). The vertical illuminance (243 lux) was lower than the horizontal illuminance (293 lux) only during the evening, as reported in Fig. 3. It is assumed that since the vertical illuminance was measured facing south, the illumination received during the afternoon was primarily oblique, which may explain the decrease with respect to the horizontal illuminance. It was observed that m-EDI was similar during mid-morning and early afternoon (1099 and 1097 m-EDI) and lower during the late afternoon (224 m-EDI). It was also observed that the efficacy ratio for different spectra; even when the vertical illuminance measured during the morning was lower than that during mid-morning, m-EDI was similar due to the CCT. This is in agreement with CIE S 026 (Table A.2).

Difference between four conditions

The influence of the curtains on the incidence of natural light in the room interior was clearly observed (Fig. 4, Fig. 5). The loss of indoor illuminance levels depends on the shaded window (west or south) and the time of day, and consequently the effective changes to measured

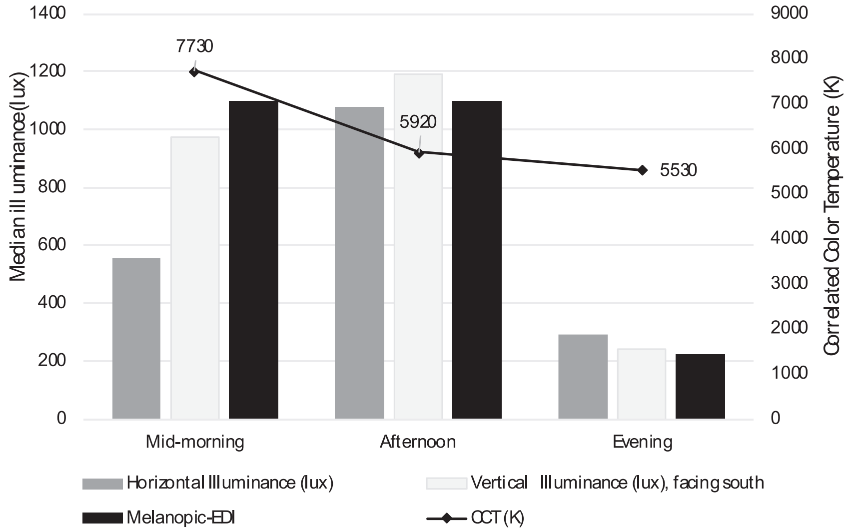

Fig. 3
Illuminance during the day

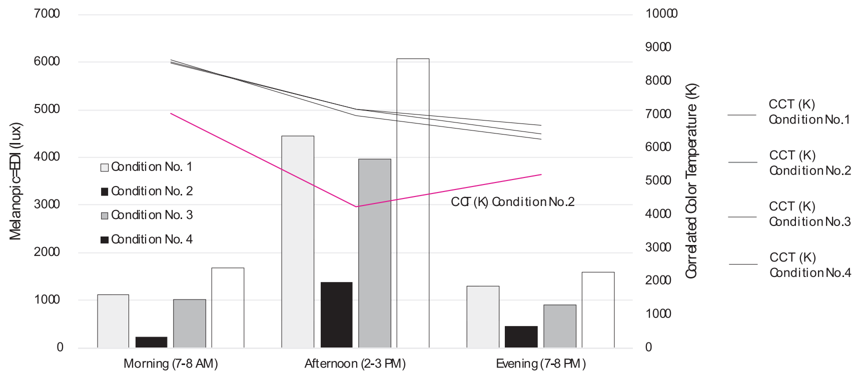

Fig. 4
Melanopic EDI during one day - southern view

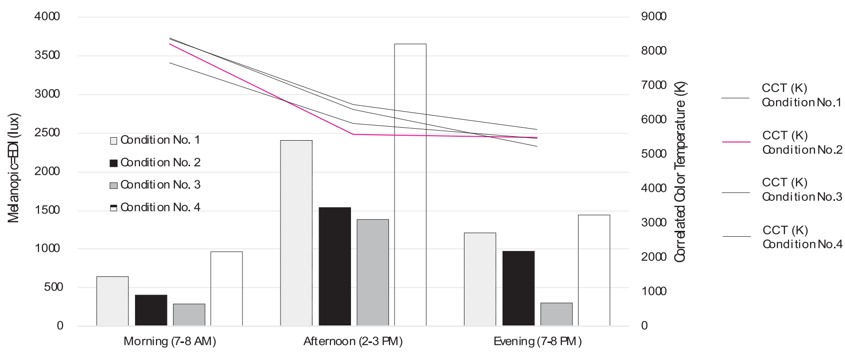

Fig. 5
Melanopic EDI during one day - western view

m-EDI.

When the direction of the field of view faced south from the observation point, closing the curtains to the south windows (*Condition No.2*) caused a significant reduction (>70%) in m-EDI at any time of the day. Closing the west curtains (*Condition No.3*) led to a decrease of less than 10% in m-EDI values. The loss of m-EDI in the field of view towards the west was similar when either the south or west curtains were closed (35-50%), except during the afternoon, when the influence of the west curtains on the effective illuminance was observed (75%).

An increase in m-EDI was also observed when the windows were fully open on both south and west facing facades (*Condition No.4*). Illuminance values increased by almost 50% during the morning and mid-afternoon with 20% increase in the evening. It can be observed that the window size and design has influence on interior daylighting; in this case the west facing windows are partially veiled by trees, explaining the difference between open and closed window conditions.

It was also observed the variation of daylight colour temperature through the day which, together with the luminous intensity, determines the m-EDI. It can be observed that curtains can modify indoor CCT, especially in direct sunlight, as shown in Fig. 4 and Fig. 5.

Melanopic ratio is reported in Table. 3 and Table. 4, which included variations throughout the day, both as a result of change to the daylight spectrum, as well as the effect of other factors such as curtains.

Luminance Analysis and the Quality of View

Luminance analysis (Fig. 6 to Fig. 11) was carried out for all *Conditions No.1* to *No.4*. Average luminance values in the field of view and vertical illuminance values were calculated.

Average luminance values and vertical illuminance values were the highest during the afternoon when the direction of view faced south from the observation point and windows were open (*Condition No. 4*). Average luminance values and vertical illuminance values were the lowest during morning when the direction of view faced south from the observation point and southern windows were shaded (*Condition No. 2*).

Although m-EDI values were the highest in both views during the afternoon with open windows, open windows caused the highest average illuminance value in the southern view. Closing windows caused a 22% reduction in average luminance value and a 28% reduction in average vertical illuminance value.

Although m-EDI values were the highest in both views with open windows, open windows resulted in large areas with higher luminance values in the southern view. It can be predicted that those large areas could cause potential glare. These areas were reduced by closing the windows or closing the west-facing curtains. When closing the curtains, there was a significant reduction of areas with higher luminance values. At the same time there was only a slight decrease in the m-EDI values

Melanopic EDI [1]	No. 1	No. 2	No. 3	No. 4
Morning	1 127	233	1 012	1 672
Afternoon	4 439	1 370	3 961	6 074
Evening	1 300	457	904	1 584
Melanopic ELR [2]				
Morning	1.53	1.42	1.53	1.53
Afternoon	1.40	1.08	1.40	1.38
Evening	1.33	1.18	1.36	1.32

Table. 3

Stimulus specification table - southern view conditions

[1] EDI equivalent daylight illuminance (in lx)

[2] ELR efficacy of luminous radiation: ELR (in mW.lm-1)

Melanopic EDI [1]	No. 1	No. 2	No. 3	No. 4
Morning	641	410	290	962
Afternoon	2 412	1 543	1 386	3 654
Evening	1 212	972	308	1 444
Melanopic ELR [2]				
Morning	1.51	1.50	1.46	1.50
Afternoon	1.32	1.23	1.28	1.30
Evening	1.24	1.21	1.24	1.18

Table. 4

Stimulus specification table - western view conditions

[1] EDI equivalent daylight illuminance (in lx)

[2] ELR efficacy of luminous radiation: ELR (in mW.lm-1)

compared to the condition with the closed windows (*Condition No.1*).

Higher luminance values were observed when windows were fully open (*Condition No.4*) throughout the whole day in both the south and west views, mainly in the afternoon (Fig. 8, Fig. 9). In particular, the values were higher at the surface of the ceiling, in comparison to the condition with windows closed and all curtains open (*Condition No.1*). This result highlights the importance of window design, the window frame size as well as the glazing configuration and specification. The afternoon southern view provides the occupant with higher values of luminance and on all horizontal surfaces in the field of view. Large differences between luminance values in the observer's field of vision can lead to discomfort glare and disabling glare. See Fig. 12 to visualise the vertical illuminance and average luminance in the field of view for the different *Conditions No.1* to *No.4*.

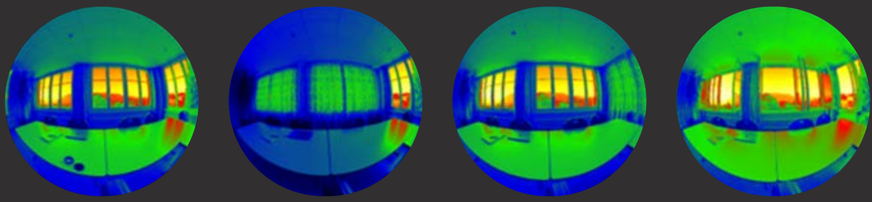

Fig. 6

Luminance maps - morning, southern view

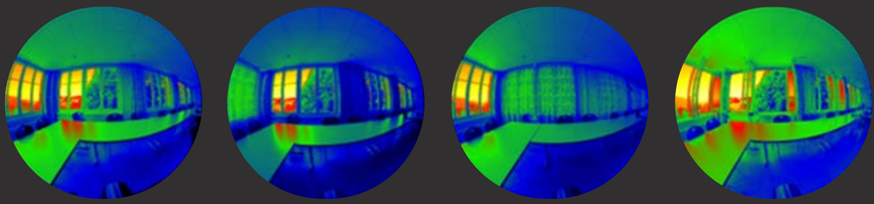

Fig. 7

Luminance maps - morning, western view

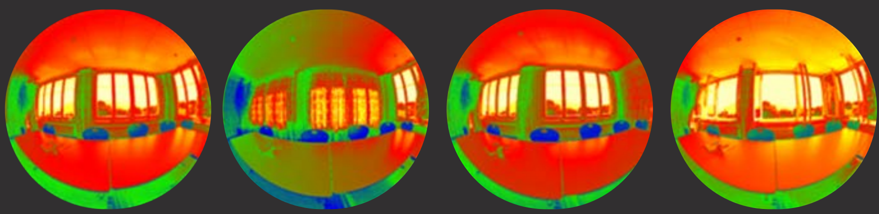

Fig. 8

Luminance maps - afternoon, southern view

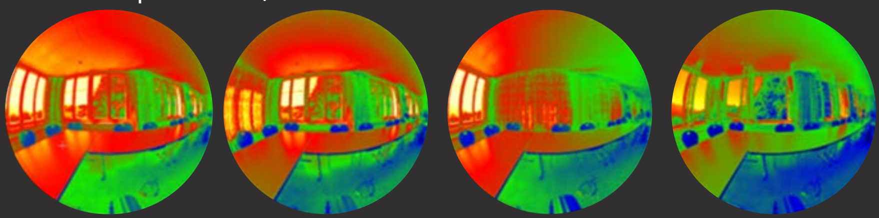

Fig. 9

Luminance maps - afternoon, western view

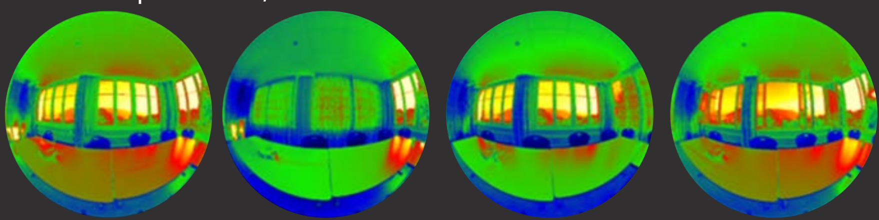

Fig. 10

Luminance maps - evening, southern view

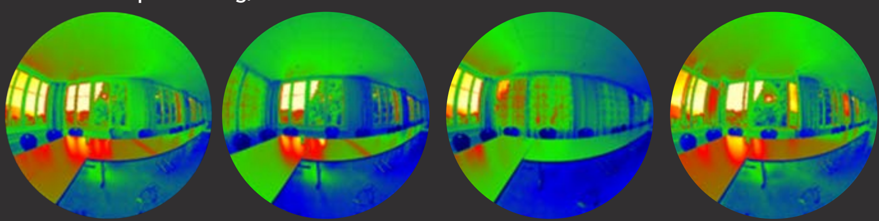

Fig. 11

Luminance maps - evening, western view

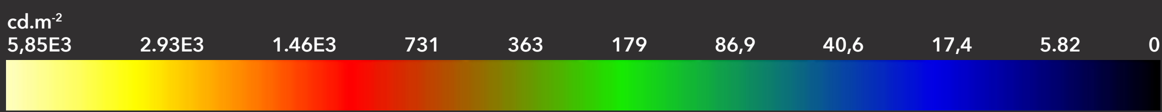

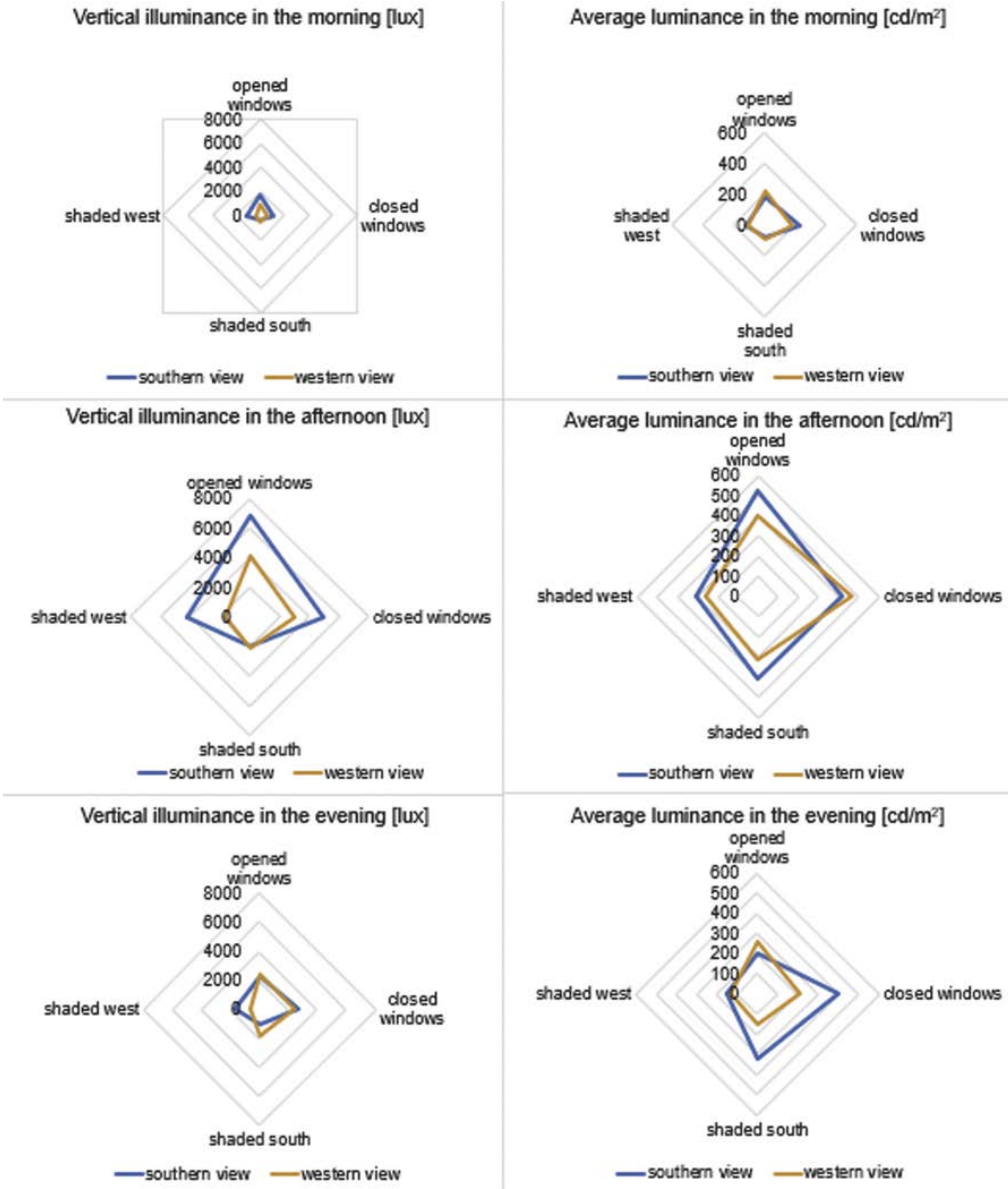

^ **Fig. 12**

Vertical illuminance and average luminance in the field of view

The quality of view in Table. 5 is defined as per EN 17037, for assessment of the view out:

(1) size of the daylight opening(s)
(2) number of layers [sky, landscape (natural/urban/horizon), ground (incl. activities)]
(3) outside distance of view
(4) width of the view [horizontal sight angle]
(5) quality of the information in the field of view

Table. 5

View		
Criteria	Southern view	Western view
1	3 windows	4 windows
2	2 (sky and landscape)	2 (sky and landscape)
3	14 km	0,5 km and less
4	Narrower	Wider (veiled by trees)
5	Subjective evaluation required	Subjective evaluation required

Assessment for view out (EN 17037)

Discussion

Considering view evaluation in accordance with the requirements of the EN 17037, the western view is rated higher than the southern view. However, the quality of view contents towards the south has a higher score compared to the partially obstructed view towards the west. The southern view includes trees with green leaves (during the summer when the study was conducted), which are low and do not obstruct the view towards Lake Geneva and the mountains beyond. The view towards the west is partially obstructed by trees with green leaves (during the summer), which are close to the building's façade. Further studies including subjective evaluation and view content analysis would need to be undertaken for a more comprehensive view assessment.

Melanopic illuminance has demonstrated to be a useful metric for predicting the circadian impact of environmental illumination (Brown, 2020). The action of daylight intensity and spectra determines, among other variables, the effect of lighting on health and wellness. This study first examined outdoor and indoor daylight illuminances where measurements demonstrated the variation of daylight throughout the day. Indoor illuminance exceeded the minimum m-EDI recommendation (250 lux) suggested by recent research (Brown, et al. 2022). The influence that window orientation and outdoor context can have on the resulting indoor illuminance was observed; outdoor illuminance, particularly on vertical surfaces, is critical for indoor daylighting design. Closing the curtains on the south-facing windows during the morning resulted in a substantial reduction (>70%) in melanopic illuminance, to levels below current guidelines, showing that the natural light captured by the west-facing windows would be insufficient to provide a healthy environment.

Changing the indoor lighting conditions, by opening or closing the curtains, made it possible to analyse the influence they have on the melanopic illuminance and the perception of brightness. The relationship between indoor illuminance and m-EDI was observed: a decrease in indoor illuminance will result in a reduction in the stimulus received by the eye. However, this stimulus will not depend only on the illuminance, but also on its spectrum. It was observed that different illuminances during the morning and afternoon (976 and 1190 lux) resulted in similar m-EDI (1099 and 1097 lux) due to variations in the daylight spectrum recorded through CCT. Blue-enriched morning light (7730 K) will result in a higher melanopic illuminance, which might have a positive effect on mood, sleep, and circadian rhythms.

While several studies have shown the importance of morning light for better sleep and the regulation of circadian rhythms, this study shows the impact that curtains can have on the provision of daylight and melanopic illuminance. This may prove significant for the elderly considering that disrupted sleep and circadian regulation contribute to loss of neural function (Mattis & Sehgal, 2016).

While internal shading is used to regulate daylighting and control glare, windows also offer views. The view from a window can affect several aspects of physical and mental wellbeing (Knoop, et.al., 2020). Views through windows maintain connection with the outdoors, sensing the time of day and the weather conditions. This can be important for an occupant's health, as it is a way of having a connection with the world – particularly for those who spend most of their time indoors – supporting psychological and physiological aspects of health (Fu et. al., 2022).

On the other hand, increasing sunlight through windows and, consequently, the increase of luminance distribution can cause glare and reduce visual acuity and comfort – curtains are often used to remediate this effect. However, the analysis of the four studied conditions highlights the impact of internal shading and window design (including frame size) on indoor daylighting and melanopic equivalent illuminance.

Indoor lighting quality was also analysed by luminance maps, showing the effect of partially closed curtains (curtains to either the south or the west facing windows) – this can significantly reduce lighting levels and modify luminance distributions. If there is a direct incidence of sunlight on the window, shading elements (either internal or external) can potentially remediate the excess brightness, provide greater adaptability, and control of the light whilst increasing user visual comfort.

Strengths, limitations, and suggestions for future research

Illuminance, light spectrum, and spatial distribution of daylight define room appearance and NIFs effects. Measurement establishes parameters for the understanding of the relationship between external and internal illuminances, and daylight performance on horizontal/vertical planes. The four internal conditions enable the possible assessment of the impact of curtains on indoor lighting, visual comfort and melanopic equivalent daylight illuminance. Measuring photopic-illuminance, m-EDI and spectrum during daytime with open or closed windows and curtains, provided a broad sample of variation.

The study analysed how the spectrum was modified by shading from internal curtains. However, the physical properties of light transmission, reflection and scattering through the curtains were not analysed. Curtains made from a variety of shading materials with different properties as well as the presence of trees with dense green vegetation adjacent to the west facing windows should both be fully considered in a more comprehensive study. Simultaneous indoor and outdoor spot measurements were not always precisely synchronised. A one-day study could not measure different weather conditions, therefore findings cannot be generalised. A wide-ranging set of weather and sky conditions must be considered to provide a broader study of the impact on melanopic illumination. Additionally, the case study room size, proportions and configuration may not be sufficiently representative of domestic settings, nor reflect the habits and preferences of occupants.

Further studies could include a more detailed analysis of seasonal cloud cover and daylighting variations. Involvement of participants could provide feedback through self-report questionnaires or qualitative interviews. This could be further enriched with the use of biosensors recording participant neuro-physiological data. The outcome of such studies could provide evidence to inform guidelines and recommendations for façade openings and shading strategies for daylight, with a more holistic approach considering visual comfort as well as health generally.

For urban dwellers, buildings and urban spaces must facilitate access to daylight for its health benefits, irrespective of age, mobility, or socio-economic circumstances.

Acknowledgement The authors would like to thank the Daylight Academy for the Interdisciplinary Summer-School "Measuring Light and illumination" (Chexbres, Switzerland), Prof Manuel Spitschan, the lecturers, teaching assistants, the opportunity to work with a group of talented participants, the ESRC DTP Cambridge, and the Charlie Bayne Travel Trust Fund. The authors express their gratitude for the guidance and advice from Prof Manuel Spitschan and Dr Lenka Maierova during the summer-school and the subsequent writing-up of this paper.

References

Blume, C., Garbazza, C., & Spitschan, M. (2019). Effects of light on human circadian rhythms, sleep and mood. Somnologie : Schlafforschung und Schlafmedizin = Somnology : sleep research and sleep medicine, 23(3), 147–156. https://doi.org/10.1007/s11818-019-00215-x

Brown, T. M. (2020). Melanopic illuminance defines the magnitude of human circadian light responses under a wide range of conditions. Journal of Pineal Research, 69(1), e12655.

Brown, T. M., Brainard, G. C., Cajochen, C., Czeisler, C. A., Hanifin, J. P., Lockley, S. W., ... & Wright Jr, K. P. (2022). Recommendations for daytime, evening, and nighttime indoor light exposure to best support physiology, sleep, and wakefulness in healthy adults. PLoS biology, 20(3), e3001571.

Cajochen, C. (2007). Alerting effects of light. Sleep medicine reviews, 11(6), 453-464.

CIE S 026:2018 CIE System for Metrology of Optical Radiation for ipRGC-Influenced Responses to Light. International Commission on Illumination (CIE). https://doi.org/10.25039/s026.2018

CIE TR 21783:2022: Light and Lighting – Integrative lighting – Non-visual effects

EN 17037:2018+A1:2021: Daylight in Buildings (Corrigendum 1 – CEN 13 October 2021 and Amendment 1 – CEN 24 August 2021).

Fu, Y., Wu, Y., Gao, W., & Hui, R. (2022). The Effect of Daylight Illumination in Nursing Buildings on Reading Comfort of Elderly Persons. Buildings, 12(2), 214

Klepeis NE, Nelson WC, Ott WR, Robinson JP, Tsang AM, Switzer P, Behar JV, Hern SC, Engelmann WH. The National Human Activity Pattern Survey (NHAPS): a resource for assessing exposure to environmental pollutants. J Expo Anal Environ Epidemiol. 2001 May-Jun;11(3):231-52. doi: 10.1038/sj.jea.7500165. PMID: 11477521.

Knoop, M., Stefani, O., Bueno, B., Matusiak, B., Hobday, R., Wirz-Justice, A., ... & Norton, B. (2020). Daylight: what makes the difference? Lighting Research & Technology, 52(3), 423-442.

Konis, K. (2018). Field evaluation of the circadian stimulus potential of daylit and non-daylit spaces in dementia care facilities. Building and Environment, 135, 112-123.

Lockley, S. W. (2010). Circadian rhythms: Influence of light in humans. In Encyclopedia of neuroscience (pp. 971-988). Elsevier.

Mattis, J., & Sehgal, A. (2016). Circadian Rhythms, Sleep, and Disorders of Aging. Trends in endocrinology and metabolism: TEM, 27(4), 192–203.

Spitschan, M., Nam, S., & Veitch, J. A. (2022). luox: Platform for calculating quantities related to light and lighting [Software]. Available from https://luox.app/.

Spitschan, M., Mead, J., Roos, C., Lowis, C., Griffiths, B., Mucur, P., Herf, M., Nam, S., & Veitch, J. A. (2022). luox: novel validated open-access and open-source web platform for calculating and sharing physiologically relevant quantities for light and lighting. Wellcome Open Res, 6, 69. doi:10.12688/wellcomeopenres.16595.3

Spitschan, M., Stefani, O., Blattner, P., Gronfier, C., Lockley, S., & Lucas, R. (2019). How to Report Light Exposure in Human Chronobiology and Sleep Research Experiments. Clocks & Sleep, 1(3), 280–289. MDPI AG. Retrieved from http://dx.doi.org/10.3390/clockssleep1030024

UN World Urbanization Prospects: The 2018 Revision.

Vetter, C., Pattison, P. M., Houser, K., Herf, M., Phillips, A. J., Wright, K. P., ... & Glickman, G. (2022). A review of human physiological responses to light: Implications for the development of integrative lighting solutions. Leukos, 18(3), 387-414.

World Health Organization. 2017, Demographic Change and Healthy Ageing.

Wirz-Justice, A., Skene, D., & Münch, M. (2021). The relevance of daylight for humans. Biochemical Pharmacology, 191, 114304.

Project Report 3

Measuring light exposure during sleep using a light dosimeter

Vaishali Vinod

Measuring Light Exposure During Sleep Using a Light Dosimeter

Vaishali Vinod

Artificial Light at Night (ALAN) exposure is known to interrupt sleep, thereby potentially negatively impacting human health. There is increasing research studying the effects of different light spectra on sleep. The health effects of ALAN do not only depend on the intensity of light but also on factors such as its exposure length and spectral properties, which can be measured with the light dosimeter. The light dosimeter is a miniature device that measures the light exposure of an individual. Here, this device is assessed for its use in measuring light properties at night during wakefulness and sleep. The light dosimeter was attached to the participant's shirt collar at night while being exposed to artificial light from a laptop screen in a dark room. The device was able to detect the light stimulus throughout the night. Thus, this study suggests the use of light dosimeters in studying light exposure also at night during sleep.

Introduction

Light is one of the major cues for the circadian rhythm. In the present-day lifestyle, humans tend to rely on artificial light, especially at night. Artificial Light at Night (ALAN) can inhibit nocturnal melatonin production and cause a phase shift in the circadian rhythm (Smolensky et al., 2015). This is associated with various diseases that affect sleep, cognition, and metabolism (Touitou et al., 2017). Over the years, ALAN exposure has been increasing in different populations, especially with a culture indulging in digital entertainment before bedtime. Light from TV or computer screens is enriched with short-wavelength or "blue" light that suppresses melatonin production, thereby negatively affecting sleep (Chellappa et al., 2013). A study has shown that light with a higher color temperature suppressed melatonin production more than light with a lower color temperature (Santhi et al., 2012).

Sleep and its disturbances are objectively assessed with polysomnography (PSG), which can also be done in an ambulatory setting. PSG is a multi-parametric approach that records for instance brain waves, heart rate, breathing, blood oxygen levels, eye movements and leg movements during sleep. PSG is considered a gold standard to assess the quality of sleep as it provides a comprehensive picture of the various sleep stages and bodily functions. Of the many factors that can affect sleep quality, light input at bedtime plays a major role. Hence, to understand the correlation between sleep and light exposure at night, it can be beneficial to couple PSG with a device to measure light. Light exposure can be measured using the light dosimeter which not only records the amount of light but also the light spectra an individual is exposed to.

The light dosimeter is a compact, portable device used to study the visual and non-visual effects of light, developed by the Lucerne University of Applied Sciences and Arts (HSLU) (Stampfli et al., 2021). It is designed to measure light exposure at eye level and can be conveniently attached to an eyeglass frame. This device records the composition of light exposure and parameters such as optic irradiance, illuminance, and correlated color temperature.

Though the device was designed to be wearable and measure light in day-to-day functions, its properties could be beneficial in estimating light exposure at night and during sleep. In this study, the non-visual effects of ALAN are measured using the light dosimeter and estimate the extent of application of the device in collecting light data in sleep studies.

Objectives

To assess the practical application of the light dosimeter measuring light exposure during sleep.

Material and Methods

This study was carried out in one participant who wore the light dosimeter near the shirt collar for two nights. During night 1, the participant slept in a dark room and during night 2, the participant slept in a dark room with light from a laptop screen directly facing the participant. The dosimeter collected light measurements every 10 seconds. The device was activated on night 1 and the data was collected throughout the following day and night 2. Subsequently, the data was downloaded and analyzed in the Lido Studio software.

Results

The above plots were obtained from Lido Studio. In the plots, night 1 is represented with the date 2022-08-16 and night 2 with 2022-08-17, along with the timestamp of data collection.

The plots show light input throughout the period of time the participant was wearing the light dosimeter. During night 1, when the

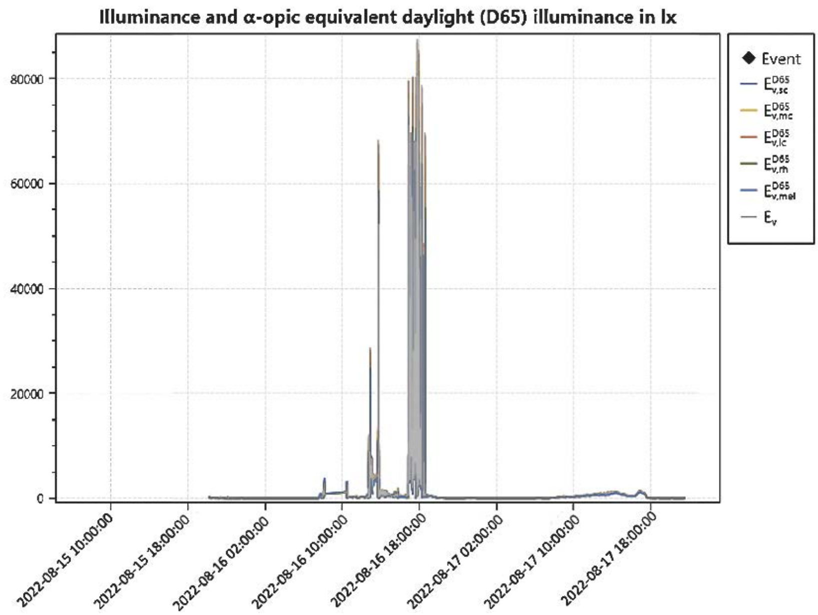

Fig. 1

Illuminance and α-opic equivalent daylight (D65) illuminance in lx for the three cone types (Esc, Emc, Elc.), rods, and intrinsically photosensitive retinal ganglion cells (ipRGCs, Ev,mel). The graph shows very low illuminance measured by the device at both nights.

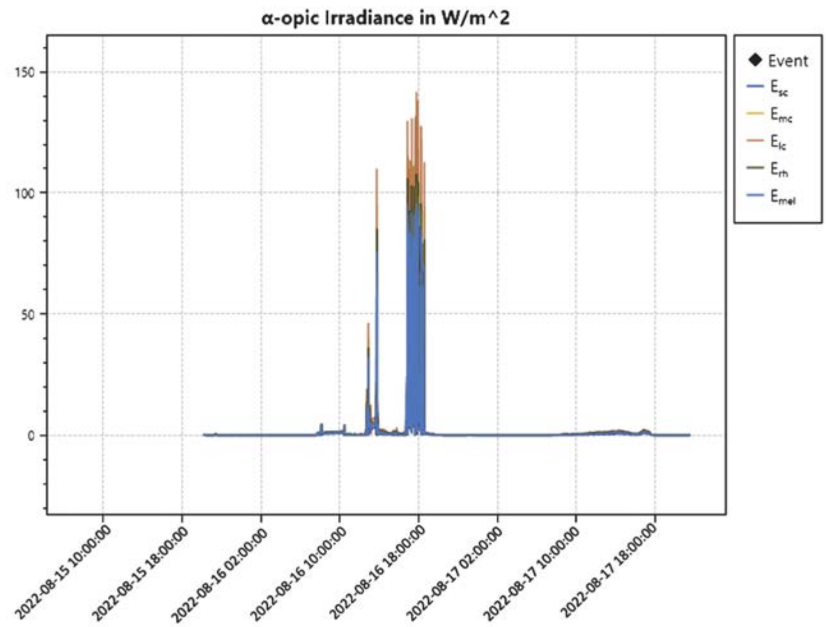

Fig. 2

α-opic irradiance in W/m2 for the three cone types (Esc, Emc, Elc.), rods, and intrinsically photosensitive retinal ganglion cells (ipRGCs, Emel).

participant was sleeping in the dark, light input was not detected. On the following day, the daylight exposure of the participant was measured but this data is not relevant to this study. On night 2, the light from the laptop screen was measured when the participant was sleeping. A difference in the peaks is observed between data measured from daylight and light at night.

107

This study aimed to assess the application of a "light dosimeter" device in sleep studies that measure sleep quality in the presence of artificial light throughout the night. The light dosimeter is portable and compact enough to be worn by an individual even during sleep. It is convenient to collect light measurements without being a hindrance to the individual's everyday tasks. From the results, the amount and composition of light exposed by the participant during the two nights are measured.

The data of light measured during the day was not considered for this study but can be considered as a reference to show the differences in the spectral composition of daylight and artificial light at night. The illuminance measured on both nights was extremely low, even during the night of artificial light exposure.

The correlated color temperature (Fig. 3) was higher in light from the laptop screen compared to that of daylight. The light measurement was not consistent for night 2 although there was a constant light stimulus (cf. Fig. 3). This might be because the position of the light dosimeter changed as the participant changed sleep positions and might not have been directed towards the light source.

The light dosimeter combined with polysomnography (PSG) could help understand the effect of light at night during sleep. For instance, to study volunteers who sleep with a night lamp on, or those who fall asleep with their TV or computer screens on. Sleep quality can be studied with parameters such as sleep fragmentation, sleep onset latency, and the arousal index.

A similar study design with PSG could be employed to study the different light exposure conditions and their effects on memory and cognition. The light dosimeter can also be used to measure light exposure in shift workers and relate it to their sleep quality. The device can be suitably designed for ease of wearability during sleep. It can also be applied to explore hypotheses on the non-visual effects of light differing between people of different ancestry. A deeper understanding of mechanisms of how different light spectra influences health in different populations can help develop "circadian-clock friendly" lighting solutions.

Light is one of the most important environmental factors affecting sleep. While daylight has many benefits for health, artificial light at night (ALAN) alters the circadian rhythm causing a phase shift and suppressing the production of melatonin. Many studies aim to understand the mechanisms of what properties of artificial light cause sleep disturbances. Light dosimeters can measure the spectral properties of light and this study suggests its usefulness in sleep research.

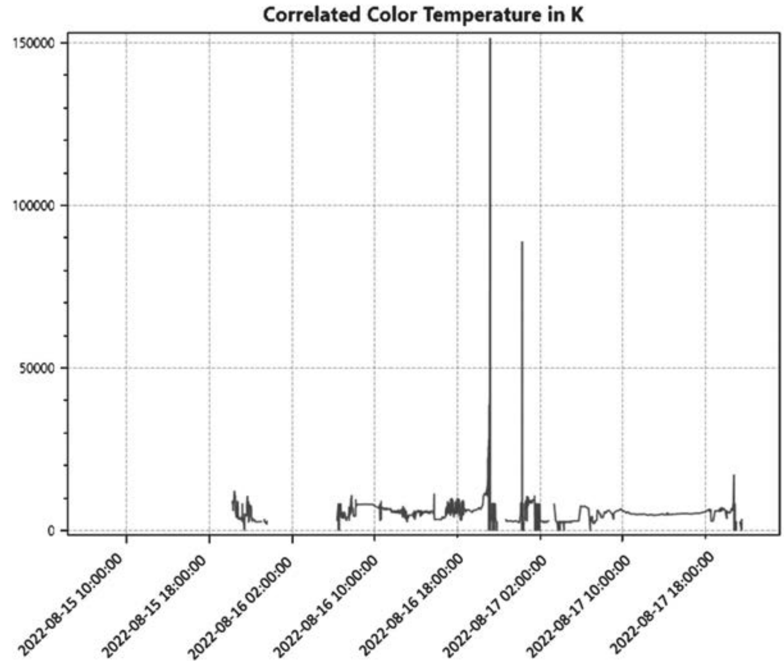

Fig. 3

Plot showing Correlated Color Temperature in K, recorded for two nights, one without artificial light (Night 1) and one with artificial light exposure (Night 2).

Acknowledgement This project was made possible thanks to the valuable inputs from Prof. Dr. Manuel Spitschan, faculty members, teaching assistants and my fellow teammates Marzieh Nazari, Philip McAdams and Samuel Ponting. I would like to extend my sincere gratitude to the Daylight Academy and the whole team of the summer school for their guidance, support and spirit.

References

Chellappa, S. L., Steiner, R., Oelhafen, P., Lang, D., Götz, T., Krebs, J., & Cajochen, C. (2013). Acute exposure to evening blue-enriched light impacts on human sleep. Journal of sleep research, 22(5), 573–580. https://doi.org/10.1111/jsr.12050

Cho, Y., Ryu, S. H., Lee, B. R., Kim, K. H., Lee, E., & Choi, J. (2015). Effects of artificial light at night on human health: A literature review of observational and experimental studies applied to exposure assessment. Chronobiology international, 32(9), 1294–1310. https://doi.org/10.3109/07420528.2015.1073158

Santhi, N., Thorne, H. C., van der Veen, D. R., Johnsen, S., Mills, S. L., Hommes, V., Schlangen, L. J., Archer, S. N., & Dijk, D. J. (2012). The spectral composition of evening light and individual differences in the suppression of melatonin and delay of sleep in humans. Journal of pineal research, 53(1), 47–59. https://doi.org/10.1111/j.1600-079X.2011.00970.x

Smolensky, M. H., Sackett-Lundeen, L. L., & Portaluppi, F. (2015). Nocturnal light pollution and underexposure to daytime sunlight: Complementary mechanisms of circadian disruption and related diseases. Chronobiology international, 32(8), 1029–1048. https://doi.org/10.3109/07420528.2015.1072002

Stampfli, JR, Lazar, R., Spitschan, M., Schrader, B., di Battista, C., Häfliger, R., Schälli, O., Wichmann, G., Zumbühl, C., Blattner, P. and Cajochen, C. The Light-Dosimeter - A New Device to Help Advance Research on The Non-visual Responses to Light. In: Proceedings of the Conference CIE 2021. International Commission on Illumination, CIE, December 2021, https://doi.org/10.25039/x48.2021.op18

Touitou, Y., Reinberg, A., & Touitou, D. (2017). Association between light at night, melatonin secretion, sleep deprivation, and the internal clock: Health impacts and mechanisms of circadian disruption. Life sciences, 173, 94–106. https://doi.org/10.1016/j.lfs.2017.02.008


In August 2022 the Daylight Academy Interdisciplinary Summer School "Measuring Light and Illumination" brought together a diverse group of students and lecturers to learn about measuring light and its effects on human health. Located in Chexbres, Switzerland, with a stunning view of Lake Geneva, the school drew inspiration from the cyanometer – an 18th-century instrument used to measure the colour of the sky by visual inspection. Our location in Switzerland reflects where de Saussure used his instrument: On his tours onto Mont Blanc.

Light is not just a source of illumination but a force that shapes our daily rhythms, from the moment we wake up to the time we go to sleep. This book summarises our enlightening experiences and learnings during our time in Chexbres and invites you to join and relive our light journey through time, space and disciplines. This interdisciplinary summer school showed us that studying light is not just a technical pursuit but a journey of discovery that connects us to nature, art and our own humanity.